university of groningen / faculty of science and engineering

Bachelor Research Project in Physics

Simplified Models for Dark Matter-Neutrino Interactions

Author: Ivo Gabrovski

Supervisor: Simone Biondini

Second Examiner: Daniël Boer

Abstract

In this thesis we begin with a brief review on Dark Matter and neutrino physics, which serves as a broad introduction to the topic and what follows. In the main part of the thesis, we take a closer look at a scenario where Dark Matter interacts weakly with neutrinos. More specifically, Dark Matter is taken to be a Weakly Interacting Massive Dirac fermion, which interacts with neutral leptons via a complex scalar mediator. Elastic scattering and self-annihilation of Dark Matter are examined closely by construction and computation of Feynman diagrams, amplitudes, and respective cross-sections of the interactions. The final parameter space of the model consists of the masses of the newly introduced Dark Matter and mediator particles and the coupling strength parameter of the interaction. The model is subsequently constrained by the most recent cosmological observations and analysis of the Cosmic Microwave Background by the Planck Collaboration. The parameter space is restricted greatly and the restrictions result in a model, which fits very well with current expectations and predictions for Dark Matter interactions on the scale of WIMPs. Possible signatures in direct and indirect detection are briefly discussed.

June 2020

Contents

Chapter I

Preliminaries

1 Introduction and Outline

In the last four decades, many scientists from all around the globe have joined forces to tackle the so-called Dark Matter problem. Various indirect observational evidence suggest the fact that an enormous matter-originating energy density should be present in the Universe. However, no one has detected it directly even though it has been the centre of scientific attention for almost half a century. Clearly, the theory of the Standard Model (SM) does not explain or describe the observed reality in a complete way and a more general physical theory is necessary. Without tests, which could prove it wrong, a theory is just a fictional story and this is where Dark Matter causes significant problems – it is only confirmed to interact gravitationally so even though there exist many theories and some are looking promising, conclusive proof for any of them has not been found.

Another particle, which pulls Physics away from the Standard Model, is the neutrino. Despite the Standard Model accommodating the neutrino, research from the past twenty years has shown that it fails to describe fully the particle's behaviour, which is mostly due to its extremely small mass. Therefore, the neutrino is thought to be the link to a theory of Physics Beyond the Standard Model, just like Dark Matter. These two links might be completely unrelated, but it is worthy to consider the possibility where they are, in fact, related. The strongest motivation for this comes from the likelihood that Dark Matter interacts approximately around the weak scale and the Standard Model particle best known for only interacting weakly is the neutrino. Neutrinos are extremely hard to detect and extract information from, but if they turn out to interact with Dark Matter, their detection and subsequent information extraction could prove crucial to the understanding of Dark Matter.

This thesis begins with an introductory review of Dark Matter and neutrinos, the main properties and discoveries related to them, how exactly their interaction could fit in the grand scheme of things, and the mathematical tools necessary to examine them. In the main part of the thesis, we consider a simplified model of Dark Matter, in which we allow it to interact weakly with neutrinos. Moreover, we make a guess about the nature of Dark Matter by classifying it as a Dirac fermion, which interacts with neutrinos via a complex scalar mediator. An elastic scattering interaction of the two particles is studied in detail as well as an interaction where Dark Matter annihilates into neutrinos. This model contains significant simplifications and assumptions. Nonetheless, we show how its general properties and how these properties could be tested observationally. The crux of the philosophy of such simplified models is to extend the Standard Model by just the bare minimum to accommodate Dark Matter and its possible interactions with

Standard Model particles. This allows for a superficial study of general behaviour, from which valuable conclusions could be made.

In today's world, data collection is advancing with an exponential pace and it is thought that with the rise of gravitational wave astronomy and neutrino astronomy, many theories of Dark Matter will fall out or prove to give useful insights in the right direction. The ultimate goal for this thesis is to examine one model and find out exactly what certain observations would mean for it, how can it be confirmed to lead to something useful or conversely, how can it be shown that the model is a very poor description of reality and others should not be wasting their time on it in the future.

2 Background on Dark Matter

Dark Matter is a term which is loosely used to describe all matter in the Universe with unknown and non-baryonic character. It is labelled as *matter* because its density follows an inverse cubic scale law $\rho_{\mathrm{m}} \propto a^{-3}$ (as opposed to radiation for which $\rho_{\mathrm{r}} \propto a^{-4}$) and the term *dark* partially refers to its observed lack of interaction with light and electromagnetic forces in general.

Evidence for the existence of Dark Matter was first found and considered by Kelvin and Poincaré[1] in the late 19^{th} and very early 20^{th} century during their analysis of the Milky Way. Later on, in 1922, Kapteyn hinted at the existence of more matter in galaxies based on stellar velocity observations.[2] However, the first articles which led to serious considerations for the existence of Dark Matter are considered to be those of Oort[3] and Zwicky.[4] Oort, who worked in the steps of Kapteyn, observed the movement of stars around the Sun and found that their velocities were significantly different from what one would expect based on the gravitational forces of visible matter only. Similarly, Zwicky observed the dispersion velocities of individual galaxies within the Coma cluster and concluded that they did not match theoretical predictions based on the Virial theorem and gravitational potentials due to visible matter. For the next 3-4 decades these findings and the issue that they introduced stayed outside of the scientific spotlight[5,6] as they essentially came at the same time as the boom in Particle Physics.[7] It was only in the 70's when the field was re-introduced, mainly by the work of Rubin, Ford,[8] and Freeman.[9] Subsequently, it was popularised by Rubin in her paper from 1980,[10] after which the field really took off and started growing significantly.

2.1 Evidence for the Existence of Dark Matter

Nowadays, we have plenty of conclusive evidence on the existence of Dark Matter, which can be loosely divided in three scales in the Universe. These are the galaxy scale, the galaxy cluster scale, and the cosmological scale; the bottom-line is that without Dark Matter, the Universe would not look like and behave in the way it is observed to.

On the scale of galaxies, the main mechanism through which the presence of Dark Matter is surveyed is the construction and analysis of the so-called rotational curves. The aforementioned works of Kelvin, Poincaré, Kapteyn, and Oort loosely fall in this category. Rotational curves consider the circular velocity v_r of astronomical objects (of mass m) as a function of the radial distance r from the centre of the galaxy. If we consider large radial distances (so that the total mass of the galaxy M is approximately constant), we can model the rotation of the galaxy by equating the Newtonian[a] gravitational force to the centrifugal force, so that

[a] Newtonian gravity is perfectly reasonable to use on this energy scale and for this purpose

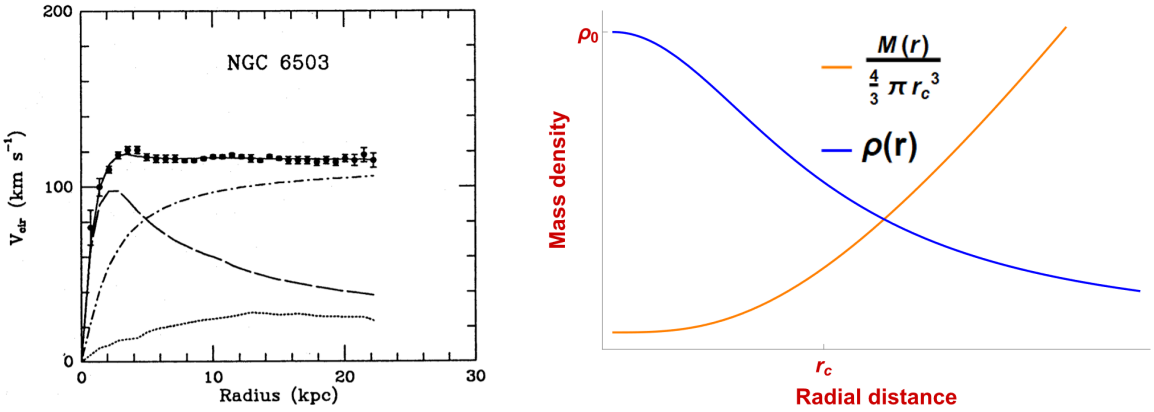

(a) (b)

Figure 2.1: **(a)** Rotational curve of the Galaxy *NGC 6503* is given by the solid line. The dashed line represents the visible matter, the dotted represents the gas, and the dot-dash represents the Dark Matter. Taken from *Begeman et al, 1991*.[12] **(b)** Rough estimate for the density distribution of Dark Matter in a Dark Halo of a spiral galaxy in dash-dot blue and the normalised full expression as in Eq. (2.2) for the enclosed mass in orange. Note: $r \gg r_c$ is of particular interest.

$$\frac{m\,v_r^2}{r} = G\frac{m\,M(r)}{r^2} \quad \Longrightarrow \quad v_r \propto \sqrt{\frac{M(r)}{r}} \propto r^{-\frac{1}{2}} \;\text{ for }\; M(r) \approx \text{const.} \tag{2.1}$$

However, observation shows that the rotational curves of most spiral galaxies stay rather flat (See Fig. 2.1a). Not all spiral galaxies necessarily follow this flatness of the rotational curve, but in all of them the velocities in the arms cannot be attributed only to gravitational interaction with visible matter.[11] If we revisit Equation (2.1), but keep in mind that the mass M has to grow with r, we can introduce a Dark Halo (i.e. a concentration of Dark Matter in a spherical shell-like manner around a galaxy). An appropriate guess for the Dark Matter density distribution[12] would be $\rho(r) = \rho_0(1 + (r/r_c)^2)^{-1}$, which is plotted in Fig. 2.1b. Now, the enclosed mass, in the limit of large radial distances, can be written like

$$\begin{aligned} M(r) &= \int_0^r \rho(r')\,dV' = 4\pi\,\rho_0 \int_0^r r'^{\,2}\left(1 + \left(\frac{r'}{r_c}\right)^2\right)^{-1} dr' = \\ &= 4\pi\,r_c^3\,\rho_0\left(\frac{r}{r_c} - \arctan\left(\frac{r}{r_c}\right)\right) \xrightarrow{r \gg r_c} 4\pi\,r_c^3\,\rho_0\left(-\frac{\pi}{2} + \frac{r}{r_c} + \mathcal{O}\left(\frac{r_c}{r}\right)\right) \\ &\approx 4\pi\,r_c^2\,r\,\rho_0\,, \end{aligned} \tag{2.2}$$

which is approximately linear in r in the limit where constant v_r is observed. This can also be seen in the plot of the full expression, which is presented in Fig. 2.1b. Substituting this $M(r)$ in Equation (2.1) indeed gives the desired result – a constant circular velocity. It should be pointed out that this halo possesses a spherical symmetry, which might be confusing at first glance since visible matter does not have that symmetry in the galaxy and is often observed to clutter in a disc. As it will be discussed further on, unlike visible matter, Dark Matter does not interact nearly as

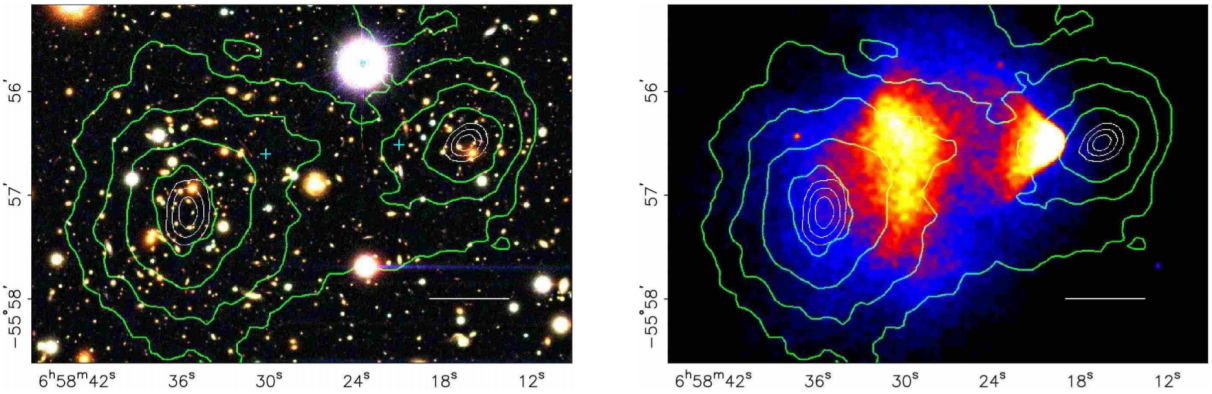

Figure 2.2: Observation of the Bullet cluster *1E0657-558*. The green contours represent mass concentration from weak gravitational lensing. The blue, red, and yellow colours represent X-ray emission intensity from intracluster plasma. Taken from *Clowe, 2006*.[22]

much with itself as visible matter does, which allows it to preserve a spherical distribution. On the other hand, visible matter dissipates energy through interaction, but has to conserve angular momentum and so the formation of discs becomes favourable. Analysis and simulations confirm this result.[13–15] There are many more ways to write down and scale the distribution in such a Dark Halo, especially when it comes to different types and sizes of galaxies.[16] The theory of Dark Halos agrees with experimental results from weak[17] and strong[18] gravitational lensing and they all point out an expected abundance of Dark Matter mass of around 4-6 times more than visible matter mass in galaxies.[6]

On the scale of galaxy clusters, one can find even more compelling evidence on the existence of Dark Matter. The works of Zwicky and others who considered dispersion velocities of galaxies within clusters fall in this category.[19, 20] Colliding clusters seem to provide even stronger evidence.[21] In particular, the collision of the Bullet cluster *1E0657-558* is thought to provide direct empirical evidence for the existence of Dark Matter.[22] In the investigation of the cluster collision, data from X-ray emission and gravitational lensing are simultaneously analysed. The former shows an abundance of gas and visible matter, which seems to 'lag behind' when compared to evidence from the latter, which shows that the main concentrations of mass in the cluster lie elsewhere (See Fig. 2.2). Analysis of this and similar clusters in general leads to the conclusion that within galaxy clusters, Dark Matter is about 5 times more abundant than visible matter.[23] Furthermore, an upper boundary for the self-interaction of Dark Matter in the present-day Universe can be derived from those observations.[22]

The final and largest scale, on which evidence for Dark Matter exists, is the cosmological scale and of particular interest are the Cosmic Microwave Background (CMB), Structure formation, and the Baryon Acoustic Oscillations (BAO). The last in the list refers to the large scale structures of baryonic matter in the present-day Universe and more specifically, the fluctuations in density of that matter. These structures can be observed today and linked to the early Universe when they were birthed by the clumping of Dark Matter[b] with baryons after recombination[c], which subsequently leads to BAO in the expanding Universe. This effect has been measured precisely and the conclusion is that it is in agreement with the prediction based on general Dark Matter models.[25–28] If Dark Matter did not exist, visible matter would not form in galaxies and clusters

[b] Assuming that Dark Matter was already present at those times

[c] An epoch taking place apprx. 370,000y after the Big-Bang, during which hydrogen atoms started forming.[24]

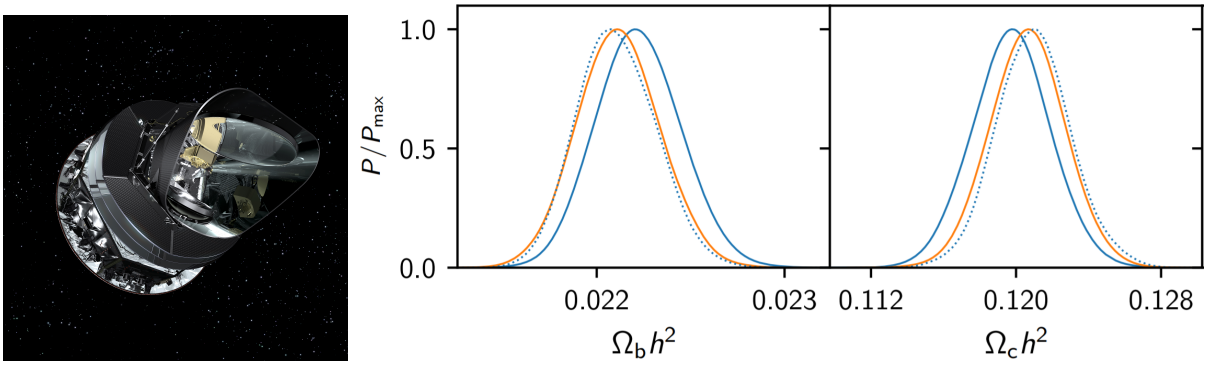

(a) (b)

Figure 2.3: **(a)** Depiction of the Planck satellite spacecraft. Taken from esa.int **(b)** Normalised probability curves for the abundance parameters of visible matter (left) and Dark Matter (right). Orange line is fit to data from 2018, while the blue line and blue-dotted are from the 2015 data collection. Taken from *Planck, 2018*[36]

due to the fact that these perturbations would not have had enough time to grow since visible matter can interact with radiation. The very early Universe was radiation dominated,[29] which signals that visible matter would be washed out and not allowed to cluster early on. However, introducing Dark Matter, which is produced before the visible matter, creates 'potential wells' in which the visible matter can later collapse more easily and thus the structure formation process is accelerated.[30]

Additionally, the CMB holds information that can be linked to the existence of Dark Matter and careful analysis can even reveal the present day abundance of Dark Matter in the Universe. The CMB was emitted shortly after the recombination epoch and it represents radiation emitted from a nearly perfect black-body of temperature $T_{\text{CMB}} = 2.725\text{K}$.[31] It is due to matter in the Universe recombining and de-ionising, thus making the Universe transparent to radiation for the first time. However, subtle anisotropies can be detected in the sky map of the CMB when decomposed into a power angular spectrum. These take the form of equally spaced peaks (See Fig. 1 from *Planck, 2016*[32]), which can be linked to the presence of ordinary matter and Dark Matter and their respective ratio of abundance in the period before the emission of the CMB. The most recent and most precise data comes from the Planck satellite (Fig. 2.3a) in 2014-15.[32,33] This leads to a composition of Dark Matter of $\Omega_{\text{DM}}h^2 = 0.1187 \pm 0.0017$ and composition of visible matter of $\Omega_{\text{VM}}h^2 = 0.02214 \pm 0.00024$ (Fig. 2.3b). Here $h = 0.697 \pm 0.024$ is the expansion rate of the Universe and $\Omega_i = \frac{\rho_i}{\rho_c}$ is the ratio of the energy density of the respective component ρ_i (i is either Dark Matter, visible matter, or Dark Energy) to the total energy density of the Universe needed for a spatially flat Universe ρ_c, which would also require $\sum_i \Omega_i \approx 1$.[34,35] Thus, results from Planck are consistent with the theory of General Relativity and the theory of Dark Matter and tie the two even closer together because the data analysis gives $\sum_i \Omega_i = 1.000 \pm 0.005$.[32] Additionally, the survey found that $4.84\% \pm 0.1\%$ of the content of the Universe is visible matter, while $25.8\% \pm 1.1\%$ is composed of Dark Matter and the rest is taking the form of Dark Energy.[33]

In conclusion, due to its nature, the CMB holds the earliest and purest information about the Universe. Features that appear in its detailed analysis can be explained very well with the theory of Dark Matter and those are further in-line with other cosmological observations. On the cosmological scale, we can see how the role of Dark Matter fits with the rest of the story

of the Universe and provides crucial context for certain events and periods within that story. Furthermore, cosmological observational data can be used to constrain any emerging Dark Matter models, including the one which we consider in this thesis as we shall see in the sections to come.

2.2 Dark Matter Candidates

So far, we have examined the evidence for the existence of Dark Matter, which we linked to the precise value for the abundance of Dark Matter in the Universe. Now, however, we have to figure out what exactly this Dark Matter is and how did it end up in the Universe in such large quantities.

First of all, it should be pointed out that many models consider the possibility that there is no extra matter, but instead the theory of gravity has to be modified. One such example is the Modified Newtonian Dynamics (MOND), which proposes that the Newtonian force be modified in a way that at high accelerations a (relative to some a_0) the theory reduces to the Newtonian theory, but at low accelerations, corresponding to the edges of a galaxy, it converges to a result, which satisfies the observed constant rotational velocity,[37] as discussed in the previous section

$$F_{\text{old}} = ma \quad \xrightarrow{\text{MOND}} \quad F_{\text{new}} = ma\,\mu(\tfrac{a}{a_0}), \qquad \begin{vmatrix} \mu(x) \xrightarrow{x\gg 1} 1 \\ \mu(x) \xrightarrow{x\ll 1} x \end{vmatrix}. \tag{2.3}$$

This theory was designed as an empirical modification, which aims to fit with the observed behaviour of spiral galaxies. However, the theory turned out to satisfy surprisingly well the dynamics of many more systems within the galaxy scale. It is only at the scale of galaxy clusters and beyond that the theory stops matching the observed reality.[38,39] It should also be pointed out that this theory is non-relativistic and there have been plenty of attempts to adapt it to relativity such as Tensor–vector–scalar gravity (TeVeS), Generalized Einstein-Aether theory (GEA), Bimetric MOND (BIMOND), etc. Many of those theories adapt well and provide accurate description of the dynamics of clusters and even agree with evidence on Large Scale Structure Formation, but none can account for the perturbations in the CMB angular power spectrum,[38,40] which leads us to believe with a rather large certainty that the Dark Matter problem needs to be approached by an introduction of a new physical particle(s).

Before we start guessing what the nature of that particle is, it is useful to revise the main properties that it must possess in order to fit with cosmological observations.[6]

I. It must be massive so that it interacts gravitationally, like observed.

II. It cannot interact strongly or electromagnetically. It could interact weakly, but the strength of that interaction has to be bounded from above, as we will see later on.

III. It must be cold or warm[d]. These terms refer to the character of the particle in the framework of Special Relativity. Cold means it is strictly non-relativistic and warm means it is cooling down and roughly on the NR boundary. Hot Dark Matter has been excluded for the most part due to analysis in Large Scale Structure formations.[41–43]

IV. The majority of Dark Matter has to be collisionless or nearly collisionless. The upper boundary on self-interactions is derived from the Bullet cluster (Fig. 2.2).[22]

V. Dark Matter has to either be a stable particle or it has to have a lifetime larger than the age of the Universe $t_{\text{DM}} \gg t_{\text{U}}$.

[d] Or at least the main component of Dark Matter must be cold/warm.[6]

Since these properties are rather general, an endless sea of Dark Matter candidates can be found. In this thesis we cover only the most fundamental and popular ones.

☐ *Neutrinos*

They are one of the most elusive and least-well understood particles of the Standard Model and since in the last two decades it has been uncovered that neutrinos are massive particles, they have been seriously considered for Dark Matter. This is largely due to their immense abundance in the Universe and the fact that they only interact weakly (and gravitationally). Nowadays, we have plenty of independent and conclusive evidence that Standard Model neutrinos cannot be Dark Matter,[44] which leads us to the hypothesis of a new kind of neutrino called a sterile neutrino.[45] Their only difference to SM neutrinos is that they do not participate in Standard Model weak interactions. Searches for a sterile neutrino Dark Matter are currently still being performed.[46]

☐ *Axions*

These particles were initially proposed in 1977[47] as a solution to the CP-symmetry violation problem. When the Dark Matter field began expanding, they were also considered as a possibility. Even though, there have been reports on indirect detection of such particles,[48] there is no conclusive evidence for this theory to be approved. Furthermore, their density is very unpredictable, which makes them hard to work around when considering them as a Dark Matter candidate.[44]

☐ *Super-symmetric particles*

The theory of super-symmetry (SUSY) revolves around the very mathematically beautiful idea that there is an additional symmetry between the two main classes of particles in the Universe – fermions and bosons. This kind of theory can introduce a plenitude of new particles, some of which have seen great interest when it comes to the search for Dark Matter.[49] The most famous candidate is the lightest super-symmetric particle – the neutralino. Other candidates of this sort include sneutrinos, gravitinos, axinos, etc. and are still viable candidates, which are being researched.[44, 50, 51]

☐ *Macroscopic candidates*

Since the beginning of the Dark Matter searches, macroscopic objects like primordial black holes have been considered.[52] Even though on some mass ranges they have been disproved, they are still a viable candidate, especially with the recent growth of gravitational wave astronomy.[6, 53–55]

☐ *WIMPs*

The Weakly Interacting Massive Particles have been a great hit among physicists and astronomers as a Dark Matter Candidate. This category is very large as the definition is very general and many super-symmetric particles like the neutralino fall in this category. The reason why WIMPs are so popular is the so-called *WIMP Miracle*. As shall be discussed during the rest of this section, allowing Dark Matter to interact weakly with itself (annihilating) can be used to determine an approximate scale on the strength of this interaction based on the abundance of Dark Matter in the Universe and it falls precisely on the expected scale.[6, 44, 56]

This list is nowhere near complete and countless other theories for light boson Dark Matter, superfluids, Little Higgs model, etc. exist. Some candidates have been dismissed and some are looking very promising, but as of today, there is absolutely zero concrete evidence that can point out that Dark Matter is a specific particle of a specific type. In this thesis, we will focus specifically on WIMPs, as we want to examine their interaction with neutrinos. Inspired by the Baryon asymmetry (significantly more abundant matter than anti-matter), asymmetric Dark Matter has also been considered seriously.[44] However, in this thesis, for simplicity, we only focus on symmetric WIMPs.

2.3 Production Mechanisms

Now that we roughly know the most general properties that this particle(s) must have and the abundance of it in the Universe, we must figure out how exactly all of that Dark Matter came to be. One hypothesis is that certain interactions with extremely low strengths (possibly with Standard Model particles as well) led to the gradual build-up of Dark Matter in the early Universe up to the point where the temperature of the Universe was too low to sustain that interaction.[57] This production mechanism is called *freeze-in*, as opposed to *freeze-out*. It is not discussed in this thesis but is, nonetheless, a fully plausible theory and its downside is that it is almost un-testable in particle detectors due to the low interactions with visible matter.[58] The aforementioned freeze-out mechanism describes Dark Matter as a thermal relic, which was once in equilibrium with the hot soup that the early Universe is (a thermal bath), but as the temperature of the Universe dropped and the Universe expanded, it decoupled from the thermal bath. For WIMPs, the exact temperature of decoupling is dependent on the Dark Matter mass. This decoupling is governed by the Boltzmann transport equation, which in this particular scenario may be written like[44,59,60]

$$\frac{dn}{dt} + 3Hn = -\langle \sigma_A v_r \rangle \left(n^2 - n_{\text{eq}}^2 \right) , \tag{2.4}$$

where n is the Dark Matter number density, $n_{\text{eq.}}$ the same density at equilibrium, H is the Hubble parameter[e] describing the expansion rate of the Universe, σ_A is the Dark Matter self-annihilation cross-section, and v_r is the relative velocity of a Dark Matter - anti-Dark Matter pair. Combined, $\langle \sigma_A v_r \rangle$ is the thermally averaged cross-section velocity product, which from now on will be known as the *thermally averaged annihilation cross-section* and will be discussed in detail in the following sections. The standard approach to simplify and solve the Boltzmann equation is to introduce a co-moving number density parameter $Y = \frac{n}{s}$, where $s = \frac{2}{45}\pi^2 g(T) T^3$ is the entropy density (conserved in thermal equilibrium so that $\dot{s} = -3Hs$) and g – the number of relativistic degrees of freedom; the mass-temperature ratio is $x = \frac{m}{T}$. Now, $\frac{dY}{dt} = \frac{dY}{dx}\frac{dx}{dt}$ and $\frac{ds}{dt} = \frac{ds}{dx}\frac{dx}{dt} = -3Hs$. Hence, in terms of the new parameters the Boltzmann equation (2.4) can be written like

$$\frac{dY}{dx} = \frac{1}{3H}\frac{ds}{dx}\langle \sigma_A v_r \rangle \left(Y^2 - Y_{\text{eq.}}^2 \right) . \tag{2.5}$$

This equation can be solved numerically (Fig. 2.4) and the results show that an increasing annihilation cross-section leads to a decrease in abundance. Additionally, the temperature

[e] The value of the Hubble parameter, determined by *Planck, 2018* is $H = 67.66 \pm 0.42 \frac{\text{km}}{s\, Mpc}$ [36]

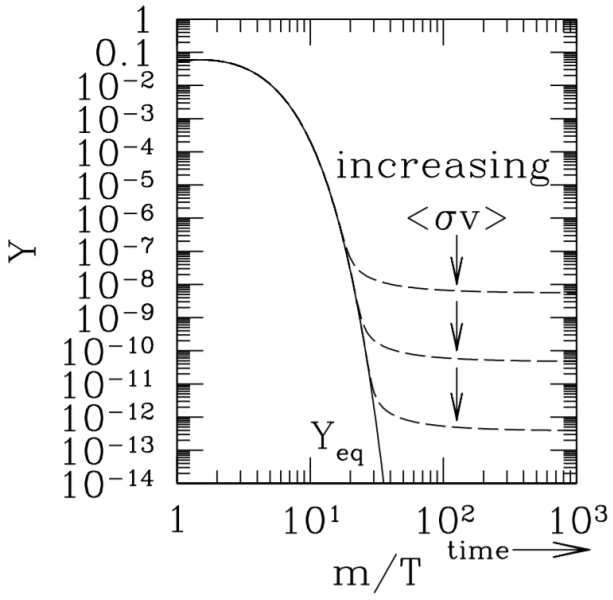

Figure 2.4: Numerical solution of the Boltzmann transport equation in the form of Eq. (2.5). Taken from *Gondolo and Gelmini, 2010*.[59]

of decoupling (which can be linked to a parameter x_F at decoupling with a known range) depends logarithmically on the Dark Matter mass only[60] and so these two can be linked with the measured abundance of Dark Matter in the Universe to give an estimate for the annihilation cross-section of $\langle \sigma_A v_r \rangle \sim 3 \times 10^{-26} \frac{\text{cm}^3}{s}$. Surprisingly, this interaction strength is very well positioned 'on the weak scale', thus contributing to the aforementioned WIMP Miracle.

3 Background on Neutrino Physics

3.1 Brief History of the Neutrino and its Properties

The particle called neutrino was first postulated 90 years ago by Wolfgang Pauli in 1930 while he was trying to explain conservation laws in beta decay. In 1956 Cowan and Reines performed the first-ever successful detection of a neutrino, thus laying the grounds for further research.[61] Since then, a lot has been accomplished in the field of lepton physics and with every answered question, many more popped up. As of 2020, the neutrino, due to its elusive nature, is considered to be one of the most mysterious and least well-understood particles in the Standard Model. However, as such, the neutrino is also considered to potentially hide the key towards a new generation physics, which usually bears the name New Physics, and immense efforts have been and are being put towards the grasp of the nature of the neutrino.

The neutrino interacts only via the weak nuclear force and possibly also the gravitational force, which is still under research. The carriers of the weak force are the $W^{\pm}$ and Z^0 bosons, which are responsible for the so-called charged current and neutral current interactions respectively.[62] The interactions that are of particular interest in astronomy are those involved in the production of cosmic neutrinos and those involved in their detection. However, interaction via a non-force carrier particle, in analogy to pions carrying out the strong nuclear force, cannot be excluded.[62]

Neutrinos are one of the most highly abundant particles in the Universe and they come

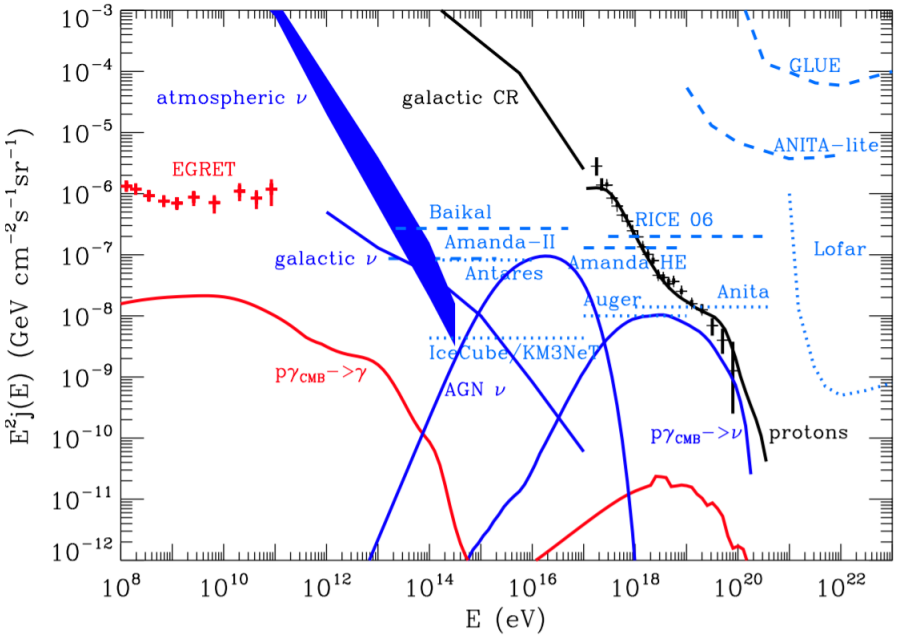

Figure 3.1: A model depicting the fluxes of astrophysical neutrinos (in blue) as functions of energy. Various neutrino detectors and their detection ranges are also shown in dashed light blue. Taken from *Sigl, 2006*.[64]

from many different sources and are available at many different energies. Significant neutrino fluxes that reach and/or pass through our planet with cosmic origin can be divided into several categories. There is a theoretical formulation and strong indirect evidence for the existence of a thermal neutrino relic density in the form of cosmic neutrino background, present since the very early Universe and produced in a similar fashion to the CMB. These neutrinos are everywhere in the Universe and possess extremely low energies of the order of magnitude $\mathcal{O}(10^{-4}\text{eV})$. Next, a significant number of neutrinos that enter the atmosphere of the Earth come from the Sun in our solar system and are thus called solar neutrinos. These come from fusion reactions within the Sun and are usually in the MeV energy range. The neutrinos in and above the GeV range are called high energy neutrinos and these can only originate from cosmic sources where immensely large amount of energy can be released.[63]

Several phenomena occur in the cosmos which are thought to produce high-energy neutrinos. All of the ones discussed here are astrophysical sources, which are thought to act as particle acceleration sites. The first and most popular ones are supernova remnants. This term represents the propagating with high velocities matter, which is ejected from a supernova, after a massive star's 'death'. Cosmic rays energy spectrum data in combination with gamma ray data has been used to show that supernova remnants are very likely to be a source of high energy cosmic rays.[65] These cosmic rays are mainly consisting of protons, which can interact with matter in/around the remnants or simply matter in the interstellar medium to produce other particles. One of the most common products of a hadron reaction are the lightest mesons – the $\pi^{\pm}$ and π^0 mesons. While the latter can potentially decay to a neutrino and anti-neutrino pair, its most likely decay channel is $\pi^0 \xrightarrow{Z^0} 2\gamma$. The charged pions, however, have most probable decay channels $\pi^+ \xrightarrow{W^+} \mu^+ + \nu_\mu$ and $\pi^- \xrightarrow{W^-} \mu^- + \bar{\nu}_\mu$.[66] In this way we see that whenever there is an emission of high energy cosmic rays, they are usually accompanied by high energy neutrinos

and gamma rays – one motivation for multi-messenger astronomy. Furthermore, high energy protons can interact with photons to produce neutrinos in their reaction.[67] A gamma ray can interact with the proton and induce a decay of the proton and multiple decay channels can result in the production of an (anti-)neutrino as an end-product. Gamma ray bursts are the most energetic electromagnetic events observed in the Universe and are a perfect source to search for such neutrinos, since they provide extremely intense and energetic photon fluxes. Gamma ray bursts can be observed due to a variety of cosmological objects and events. One group of objects that is of particular interest are the so-called active galactic nuclei, due to their ability to also accelerate cosmic rays with very high energies in the first-order Fermi mechanism.[63] As galactic nuclei have an enormous concentration of matter, it is very likely that Dark Matter is present in large abundance in and around the galactic nucleus. This would mean that in these regions Dark Matter-neutrino weak scattering would be much more likely to occur. The theoretical models of these production mechanisms suggest varying fluxes with energy for each source. The most common ones are depicted in figure 3.1. Due to these sources being present everywhere in the Universe, it can be expected that astrophysical high energy neutrinos are isotropic, and this is indeed the confirmed result.[68] In this thesis we play around with the possibility that neutrinos are also produced via a Dark Matter annihilation $\chi_{\mathrm{DM}} + \bar{\chi}_{\mathrm{DM}} \to \nu + \bar{\nu}$ channel.

3.2 Neutrino Detection

Now that we have seen how high energy neutrinos are produced, it is time to turn our heads towards detection, which is a very sophisticated task due to the extremely low interaction cross-sections of neutrinos and their lack of electric charge. Additionally, in modern-day astronomy it is not sufficient to simply detect the neutrino – if we want to extract information about its source and possible interactions with Dark Matter it might have been part in prior to detection, we must also measure additional properties like the direction of arrival, energy/momentum, etc, which makes the task even harder. The volume necessary to count the extremely small probability that a neutrino (especially on the high energy end of the spectrum) interacts with matter is on the order of cubic kilometres and above. A relatively feasible way to detect a neutrino in such a big volume is to put photodetectors in a huge volume of an approximately homogeneous dielectric medium and turn the whole volume into one big Cherenkov detector. Such are the IceCube facility, which uses Antarctic ice, and the ANTARES detector, which uses water from the Mediterranean Sea. However, one of the key components for the emission of Cherenkov light is to have a charged particle travel with relativistic velocity.[62] The high energy neutrinos travel very fast, however, they are electrically neutral. Therefore, we have to look at a charged particle that is produced due to a neutrino interaction.

Even though neutrinos can interact with other leptons, in the higher end of the energy spectrum (past GeV) neutrino-hadron interactions dominate.[69] Under a neutral current interaction, only a hadronic shower is produced, the detection of which is quite hard and even more so in a detection volume on the scale of cubic kilometres. Hence, good candidates for detection techniques are charged current interactions, where the neutrino is 'transformed' into a charged lepton. The flavour of the charged lepton depends on the flavour of the incoming neutrino and thus electrons, tauons and muons can be produced as a result of their respective neutrino interacting with a hadron. However, these three leptons possess extremely different masses and lifetimes and not all of them are as suitable for detection techniques as others. The most commonly used interactions in detectors are depicted in Fig. 3.2. The main limitations of this Cherenkov detection are that many other light sources can interfere with a measurement. Additionally, atmospheric neutrinos and muons can also have sufficiently high energies to be detected in a Cherenkov counting ex-

Figure 3.2: Two of the most common muon (anti)neutrino - hadron interactions in a detector, represented in Feynman diagrams on the nucleon scale.

periment.[64] The very nature of neutrinos makes them extremely hard to detect even in such large volumes as in the IceCube detector. There are other ways to detect high energy neutrinos as well (see figure 3.1), like the ANITA experiment, which detects radio pulses created during interaction of neutrinos with the ice in Antarctica, but they have not proven to be as useful and successful as the aforementioned two. As for lower energy neutrinos, they are also detectable by Cherenkov detectors, but Scintillators, smartly designed Calorimeters, etc. can also be used for detection.[69]

The same exact properties that make neutrinos hard to detect, also make them perfect for interaction-less propagation and quick information delivery from the source. Unlike cosmic rays, which are subject to electromagnetic forces during their galactic or extra-galactic propagation, for the most part neutrinos travel in a straight line from the source until they are detected, thus potentially providing crucial information about the source and the various physical processes that might take place there.[67] Additionally, a possible interaction with Dark Matter, which might have taken place close to the source, could potentially leave a signature on the neutrino flux, even if ever so slightly. This is generally true up to an energy of 10^{17} eV, after which the detection becomes almost impossible, due to small fluxes, but also energies so high start allowing GZK-like resonances and thus a neutrino of this energy, if it exists, would seldom reach our planet, let alone be detected.[65] Another possible neutrino production mechanism, which we will discuss in the thesis, is present day WIMP Dark Matter annihilation into neutrinos, which is thought to be likely to take place in massive stellar objects, with a lot of attention paid to the Sun and solar neutrinos.[70]

Neutrino astronomy can be considered crucial to the understanding of the cosmos, and potentially Dark Matter as well, especially when paired up with the detection of other messengers in the new field of multi-messenger astronomy. As a result, neutrino astronomy has been growing with a serious pace in the last decade and new telescopes like KM3NeT, P-ONE, and NESTOR are under construction/further development and hold high hopes for the future of neutrino astronomy.

4 Computational Basics in Quantum Field Theory

4.1 Basics of Fields and Interactions

The accepted physical theory, which accommodates both Quantum Physics and Einstein's Relativity, is known as Quantum Field Theory (QFT). As the name suggests, the theory does not deal with particles and physical objects but instead it deals mainly with fields – particles arise as natural 'ripples' or combinations of excited states of fields. In analogy to classical mechanics, the fields and their temporal and spatial evolution are governed by the variational principle of

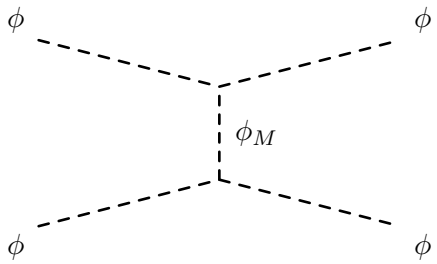

Figure 4.1: Example of a Feynman diagram for the kind of interactions that will be discussed in the main section.

least action. Every scalar field ϕ in QFT has to obey the Klein-Gordon equation.

$$(\partial_\mu \partial^\mu + m^2)\phi = 0\,, \tag{4.1}$$

where m is the rest mass of the field/particle. A Fourier transform motivates writing the general field in a Fourier series-like fashion

$$\phi(t, \boldsymbol{x}) = \int \frac{d^3\boldsymbol{p}}{(2\pi)^3\sqrt{2E_{\boldsymbol{p}}}} \left(a_{\boldsymbol{p}}\, e^{ip\cdot x} + a^\dagger_{\boldsymbol{p}}\, e^{-ip\cdot x}\right). \tag{4.2}$$

The operators $a_{\boldsymbol{p}}$ and $a^\dagger_{\boldsymbol{p}}$ turn out to satisfy the creation/annihilation operators commutation relation $[a_{\boldsymbol{p}}, a^\dagger_{\boldsymbol{q}}] = (2\pi)^3\,\delta(\boldsymbol{p}-\boldsymbol{q})$ with each other and the commutation relations $[H, a^\dagger_{\boldsymbol{p}}] = E_{\boldsymbol{p}}\, a^\dagger_{\boldsymbol{p}}$ and $[H, a_{\boldsymbol{p}}] = -E_{\boldsymbol{p}}\, a_{\boldsymbol{p}}$ with the normal-ordered Hamiltonian

$$H = \int \frac{d^3\boldsymbol{p}}{(2\pi)^3}\, E_{\boldsymbol{p}}\, a_{\boldsymbol{p}}\, a^\dagger_{\boldsymbol{p}}\,, \qquad E^2_{\boldsymbol{p}} = \boldsymbol{p}^{\,2} + m^2\,. \tag{4.3}$$

Thus, the zero-energy vacuum state $|\mathbf{0}\rangle$ can be defined by $a_{\boldsymbol{p}}|0\rangle = 0$ so that it is assigned zero energy $H|\mathbf{0}\rangle = 0$ and the creation/annihilation operators can act on it like

$$a^\dagger_{\boldsymbol{p}}\,|\mathbf{0}\rangle = |\boldsymbol{p}\,\rangle \qquad a_{\boldsymbol{p}}\,|\boldsymbol{p}\,\rangle = |\mathbf{0}\rangle \qquad a_{\boldsymbol{p}}\,|\mathbf{0}\rangle = 0 \tag{4.4}$$

to create/annihilate the state $|\boldsymbol{p}\,\rangle$. This is a momentum eigenstate, which represents a spatially (and temporally) delocalised particle with a fixed momentum $\boldsymbol{p}$. Moreover, so far, we have considered a real scalar field. In this thesis we will work with a complex scalar field and a spinor field, which have slightly different properties and operators, but the main ideas are the same.

If we now consider an interaction which converts an initial state $|i\rangle$ to a final state $|f\rangle$, we must look into their 'overlap' in order to determine the (quantum mechanical) probability amplitude for the interaction to take place. Moreover, for the interactions discussed in this thesis we are interested only in $A + B \to A + B$ elastic scattering or $A + \bar{A} \to B + \bar{B}$ annihilation in the u- or t- channels (See Fig. 4.1). In both cases, the amplitude can be written in the form of $\langle i|S|f\rangle$, where $S \in U(1)$ is the *scattering matrix*. This matrix can be very well approximated from the Dyson series if the interaction is considered as a perturbation to the theory (as is allowed here due to upper bounds on Dark Matter-neutrino interaction strengths).

$$S \simeq \sum_{n=0}^{\infty} \frac{(-i)^n}{n!} \int d^4x_1 \ldots \int d^4x_n\, T[\mathcal{H}_1 \ldots \mathcal{H}_n]\,, \tag{4.5}$$

where T is a time-ordering operator and $\mathcal{H}$ is Hamiltonian density – closely linked to the Lagrangian. Therefore, for an interaction Lagrangian of the form $\mathcal{L} = g\phi^2\phi_M$ with all fields being real scalar fields, one can construct a scattering scenario $\phi\phi \to \phi\phi$ as in Fig. 4.1. The initial momentum eigenstate can then be written as $|i\rangle = \sqrt{2E_{\boldsymbol{p}_1}}\sqrt{2E_{\boldsymbol{p}_2}}\, a^\dagger_{\boldsymbol{p}_1} a^\dagger_{\boldsymbol{p}_2} |\boldsymbol{0}\rangle$ and the final as $|f\rangle = \sqrt{2E_{\boldsymbol{p}_1\prime}}\sqrt{2E_{\boldsymbol{p}_2\prime}}\, a^\dagger_{\boldsymbol{p}_1\prime}, a^\dagger_{\boldsymbol{p}_2\prime}, |\boldsymbol{0}\rangle$.[f] Now, the diagram from Fig. 4.1 considers two distinct vertices, which denote two different spacetime points x_1 and x_2. We can consider only the g^2 term from the Dyson series and ignore the zeroth and first terms since we want actual scattering to occur. This gives

$$\langle f|S|i\rangle \simeq \frac{-g^2}{2}\langle f \,\Big|\, \int d^4x_1\, d^4x_2\, T[\phi^2(x_1)\phi_M(x_1)\,\phi^2(x_2)\phi_M(x_2)] \,\Big|\, i\rangle\,. \tag{4.6}$$

Wick's theorem[71] can be used to deal with the time-ordering operator and it gives rise to contractions of the fields. The only one, which could remain is the contraction on the mediator field, which gives rise to the Feynman propagator

$$\Delta_F(x_1 - x_2) = \int \frac{d^4k}{(2\pi)^4} \frac{ie^{-ik\cdot(x_1-x_2)}}{k^2 - M^2}\,, \tag{4.7}$$

where M and k are mass and 4-momentum of the mediator[g]. In short, aside from showcasing the role of the mediator in the interaction, the Feynman propagator also 'takes care' of the locality condition between the two vertices without caring about which one comes first on the temporal axis. Further in the computation, if the fields and states are expanded in terms of creation/annihilation operators (for fields as in Eq. (4.2)), one can start using their commutation relations to 'push' annihilation operators to act on the vacuum state, which results in a zero. The additional term, which arises due to the commutation of the operators usually gives rise to a delta function, which can be integrated. The full computation is way too long to be covered here, but the main principles have been explained and they are applied numerous times until the end result is reached.[72]

$$\langle f|S|i\rangle \simeq \frac{-g^2}{2}\langle \boldsymbol{0}|\frac{(2\pi)^4}{k^2 - M^2}\delta^{(4)}(p_1 + p_2 - p_1' - p_2')|\boldsymbol{0}\rangle = \frac{-g^2\,(2\pi)^4}{2(k^2 - M^2)}\delta^{(4)}(p_1 + p_2 - p_1' - p_2') \tag{4.8}$$

This expression is only valid for real scalar mediated real scalar-real scalar scattering. However, other variations of scattering (as we will see later) have to be computed in a very similar fashion with the only difference being that the definitions of the fields change in terms of operators and sometimes there are additional objects like spinor representations or other operators from the Lagrangian, which get translated to the final result. To reduce the length of the computation, the so-called Feynman rules[73] can be used to directly 'unpack' the amplitude from the diagram and the Lagrangian. Furthermore, it should be stated that the scattering amplitude can be expressed like $S = (2\pi)^4\delta^{(4)}(p_i - p_f)\mathcal{M}$ and $\mathcal{M}$ is known as the Feynman invariant amplitude.

The last step, which needs to be taken, is to make the link between a scattering amplitude and a scattering cross-section, which is the actual physically measurable quantity. A cross-section σ measures the probability that particles collide/interact when two beams cross or in an equation, $N = \sigma F$ where N is the number of events per unit time and F is the particle flux. We have

[f] The factors $\sqrt{2E}$ arise from normalisation requirements of the states.

[g] The momentum can be expressed in terms of the already known momenta due to conservation laws at the vertices

the possibility to compute a more useful and easier to work with quantity – the differential cross-section, which considers all outcomes "differentially" and it can be written like

$$d\sigma = \frac{\text{Differential probability}}{\text{Unit time} \times \text{Unit flux}} \tag{4.9}$$

The differential probability per unit time T can be written in terms of the known probabilities, the unit time T, the volume in which the interactions takes place V (defined by beam dimensions in colliders usually), and an infinitesimal volume in momentum space for each final state like[72]

$$\begin{aligned} P &= \frac{|\langle f|S|i\rangle|^2}{\langle f|f\rangle\langle i|i\rangle}\frac{1}{T}\prod_{\text{final states}} V\frac{d^3p}{(2\pi)^3} = \\ &= \frac{|\mathcal{M}|^2}{T}\left((2\pi)^4\delta^{(4)}(p_i - p_f)\right)^2 \prod_{\text{in. st.}}\left(\frac{1}{2E(2\pi)^3\delta^{(3)}(0)}\right)\prod_{\text{fin. st.}}\left(\frac{1}{2E(2\pi)^3\delta^{(3)}(0)}V\frac{d^3p}{(2\pi)^3}\right). \end{aligned} \tag{4.10}$$

The expression at hand is quite lengthy, but it can be simplified by noting that the delta function can be interpreted as the interaction volume for a single interaction[72] so that $(2\pi)^3\delta^{(3)}(0) = V$ and $(2\pi)^4\delta^{(4)}(0) = VT$. With that in mind, the expression can be simplified significantly to give

$$P = \frac{|\mathcal{M}|^2}{4E_{p_1}E_{p_2}V}(2\pi)^4\delta^{(4)}(p_i - p_f)\prod_{i=1}^{2}\left(\frac{d^3p_i'}{(2\pi)^3}\frac{1}{2E_{p_i'}}\right), \tag{4.11}$$

and now the flux F can be written in terms of the incoming particles' velocities and the aforementioned volume like $F = \frac{|\boldsymbol{v}_1 - \boldsymbol{v}_2|}{V}$. The final result for the differential cross-section follows from substitution and we will see later on how we can reshape it further.

4.2 Some Useful Properties of Fermionic Fields

In the previous subsection, we saw that every field in QFT has to satisfy the Klein-Gordon equation. In addition, there are fields corresponding to (anti)particles called fermions, which have to satisfy an additional equation – the Dirac equation.

$$(i\partial\!\!\!/ - m)\psi = 0 \tag{4.12}$$

Here $\partial\!\!\!/ = \gamma^\mu\partial_\mu$ and γ^μ are the Dirac matrices (or gamma matrices), defined by the anti-commutation relation $\{\gamma^\mu, \gamma^\nu\} = 2\eta^{\mu\nu}\mathbb{1}_4$. $[\eta]_{\nu\mu} = \begin{bmatrix} 1 & 0 & 0 & 0 \\ 0 & -1 & 0 & 0 \\ 0 & 0 & -1 & 0 \\ 0 & 0 & 0 & -1 \end{bmatrix}$ is the Minkowski metric. These are the basic mathematical tools needed to work with fermionic fields. If we allow the field to be written as $\psi = u(\boldsymbol{p})e^{-ip\cdot x}$ or $\psi = v(\boldsymbol{p})e^{+ip\cdot x}$, then we can solve the Dirac equation like[72]

$$u^s(\boldsymbol{p}) = \begin{bmatrix} \sqrt{p\cdot\sigma}\,\xi^s \\ \sqrt{p\cdot\bar{\sigma}}\,\xi^s \end{bmatrix}, \quad v^s(\boldsymbol{p}) = \begin{bmatrix} \sqrt{p\cdot\sigma}\,\eta^s \\ -\sqrt{p\cdot\bar{\sigma}}\,\eta^s \end{bmatrix}; \qquad \begin{aligned} \sigma^\mu &= (1, \sigma_i) \\ \bar{\sigma}^\mu &= (1, -\sigma_i) \end{aligned}, \tag{4.13}$$

where $\sigma_i \in \mathbb{C}^{2\times 2}$ are the usual Pauli matrices and η, $\xi \in \mathbb{C}^2$ are spinors satisfying normalisation $\eta^{\dagger,s}\eta^r = \delta_{r,s}$, $\xi^{\dagger,s}\xi^r = \delta_{r,s}$ and therefore also $\sum_{s=1}^{2}\xi^s\xi^{\dagger,s} = \mathbb{1}_2$. The r, s indices denote helicity of the spinor. It turns out that unlike scalar fields, fermionic fields act a little differently under Lorentz transformations and simply taking $\psi^\dagger\psi$ does not produce an object, which is invariant

under these transformations due to the nature of spinor representations. Instead, a Dirac conjugate (or adjoint) can be defined like $\bar{\psi} = \psi^\dagger \gamma^0$ with the zeroth Dirac matrix and now the product $\bar{\psi}\psi$ is indeed a Lorentz scalar. As a matter of fact, a few more Lorentz invariant objects can be constructed in a similar way.[72] A very useful outer product of these spinors, which we will use later on, is the following.

$$\sum_{s=1}^{2} \bar{u}^s(\boldsymbol{p}) u^s(\boldsymbol{p}) = \sum_{s=1}^{2} \begin{bmatrix} \sqrt{p\cdot\sigma}\,\xi^{\dagger,s} & \sqrt{p\cdot\bar{\sigma}}\,\xi^{\dagger,s} \end{bmatrix} \begin{bmatrix} 0 & \mathbb{1}_2 \\ \mathbb{1}_2 & 0 \end{bmatrix} \begin{bmatrix} \sqrt{p\cdot\sigma}\,\xi^{s} \\ \sqrt{p\cdot\bar{\sigma}}\,\xi^{s} \end{bmatrix} =$$

$$= \begin{bmatrix} m\,\mathbb{1}_2 & p\cdot\sigma \\ p\cdot\bar{\sigma} & m\,\mathbb{1}_2 \end{bmatrix} = \not{p} + m\mathbb{1}_4 \qquad \text{Similarly,} \quad \sum_{s=1}^{2} v^s(\boldsymbol{p})\bar{v}^s(\boldsymbol{p}) = \not{p} - m\mathbb{1}_4\,. \tag{4.14}$$

We now know what condition the Dirac equation imposes on the spinor field so we can turn back to the Klein-Gordon equation and its Fourier modes. This allows us to again write the spinor field as a sum of plane waves and helicities. In this notation, we see how the current (anti)particle creation and annihilation operators are associated with very specific spinors. It should be noted that fermionic operators are anti-commuting, unlike bosonic ones.

$$\psi(x) = \sum_s \int \frac{d^3p}{(2\pi)^3\sqrt{2E_{\boldsymbol{p}}}} \left(b^s_{\boldsymbol{p}}\, u^s(\boldsymbol{p}) e^{-ip\cdot x} + d^{\dagger,s}_{\boldsymbol{p}}\, v^s(\boldsymbol{p}) e^{+ip\cdot x} \right) \tag{4.15}$$

5 Introduction to the Model and Motivation for It

In the last three decades very detailed and in-depth searches for Dark Matter have proven to be in a sense futile. Even though new properties and relations of Dark Matter with the rest of the Universe have been revealed and studied in detail, Dark Matter remains just as mysterious nowadays as it was forty and more years ago, which may have been the cause of slight despair in the field. Nevertheless, it is believed that the rise of multi-messenger astronomy and gravitational wave astronomy could hold the key to tackling the Dark Matter problem in the near future.[74] Even though collisionless Dark Matter has been the more popular topic in the past decades, there is no concrete evidence for that, and we should still accept and consider the near-collisionless scenario. Furthermore, Dark Matter has to have some interaction, in order to be produced in the early Universe and it would be convenient if a similar interaction takes place today.[75]

In this thesis we want to study specifically the possible interactions of Dark Matter with neutrinos. This is a sub-field of particular interest as Dark Matter has been hypothesised to be a thermal relic of the early Universe, just like neutrinos. Also, both are thought to be present in the cosmos with a relatively large density, thus making interactions between those two practically mandatory should they be interacting in the first place. As mentioned above, in this thesis we focus on the so-called Weakly Interacting Massive Particles as this is the most sensible way to allow interactions of Dark Matter with neutrinos. Additionally, as also discussed above, new generation of neutrino detectors are on the way and in general, neutrino astronomy has been rapidly on the rise in the past decade. Therefore, if neutrinos do in fact interact with Dark Matter, it is believed that detailed data collection and analysis of neutrino fluxes from different sources could reveal crucial features about the nature of Dark Matter due to interaction beyond the Standard Model. Even if a direct signature detection is not made, analysis of cosmological neutrino behaviour can still be used to greatly cut through the parameter space of any theory that includes Dark Matter-neutrino interactions, which can turn out to be a useful guidance tool.[75] We will also see this discussed further with more concrete examples later on in the

Figure 5.1: A diagram depicting the most popular theories, proposed as solutions to the Dark Matter problem. The region of this diagram in which this thesis focuses is circled in red. Original image taken from *Bertone, 2018*[74]

.

thesis. Another significant reason for the choice of neutrinos is that they have been linked to beyond the Standard Model Physics, which Dark Matter has to fit in as well.[76] In other words, the rest of the Standard Model particles are understood to a higher degree, which allows for a more conclusive evidence on their lack of interaction with Dark Matter. Naturally, if one wants to examine interactions between Dark Matter and neutrinos, an extension to the Standard Model has to be made, which would accommodate them. This is precisely what the following chapter treats.

Chapter II

Construction and Main Analysis of a Dark Matter Model

6 The Dirac Dark Matter Model

In order to examine the possibility where a neutrino can interact with Dark Matter, we need to make use of a certain mathematics-based theory that will allow us to start from the most basic descriptions of the particles and arrive at a measurable observable. In this case, the goal-observable is a cross-section and the theory which we will use is Quantum Field Theory since it allows us to examine relativistic Physics on the particle scale. The biggest distinction that can be made between groups of particles in QFT is their intrinsic spin and how the particle is represented based on that. We know that the spin of the neutrino is spin-$\frac{1}{2}$ as it is a lepton,[62] but we do not know anything about the Dark Matter WIMP particle or the mediator particle that mediates the interaction.

6.1 Components

We will now proceed to create a toy model, which will only take into account the three mentioned particles only and exclude the rest of the Standard Model and non-SM particles and interactions [a]. The choice that we make for the first particle in this model is to consider a fermionic spin-$\frac{1}{2}$ Dirac Dark Matter particle. This allows us to write down the Lagrangian (density) of the Dark Matter as explained in Chapter I as

$$\mathcal{L}_{\text{DM}} = \bar{\chi}(x)\left(i\partial\!\!\!/ - m\right)\chi(x)\,, \tag{6.1}$$

where m is the mass of the Dark Matter particle and

$$\begin{aligned}\chi(t,\boldsymbol{x}) &= \sum_s \int \frac{d^3\boldsymbol{p}}{(2\pi)^3\sqrt{2E_{\boldsymbol{p}}}}\left(B^s_{\boldsymbol{p}}\,U^s(\boldsymbol{p})e^{-ip\cdot x} + D^{\dagger,s}_{\boldsymbol{p}}\,V^s(\boldsymbol{p})e^{+ip\cdot x}\right)\\ \bar{\chi}(t,\boldsymbol{x}) &= \sum_s \int \frac{d^3\boldsymbol{p}}{(2\pi)^3\sqrt{2E_{\boldsymbol{p}}}}\left(B^{\dagger,s}_{\boldsymbol{p}}\,\bar{U}^s(\boldsymbol{p})e^{+ip\cdot x} + D^s_{\boldsymbol{p}}\,\bar{V}^s(\boldsymbol{p})e^{-ip\cdot x}\right)\end{aligned} \tag{6.2}$$

represent the Dark Matter field and its Dirac conjugate as a sum of plane waves. In this representation, the particle creation/annihilation operators are given by B and $B^\dagger$ and the anti-particle

[a] Of course, the massive property of DM and the mediator signal for mixing with the Higgs boson, but it will be ignored for the most part of the thesis.

operators are D and $D^\dagger$. As previously covered, these can act on the vacuum state $|0\rangle$ to create or annihilate a delocalised Dark Matter particle state with momentum $\boldsymbol{p}$ and spin s (up/down).[72]

$$B^{\dagger,s}_{\boldsymbol{p}}|0\rangle = |\boldsymbol{p}, s\rangle \qquad B_{\boldsymbol{p}}|0\rangle = 0 \qquad D^{\dagger,r}_{\boldsymbol{p}}|0\rangle = |\boldsymbol{p}, r\rangle \qquad D_{\boldsymbol{p}}|0\rangle = 0 \tag{6.3}$$

$U(\boldsymbol{p})$ and $V(\boldsymbol{p})$ are the spinors corresponding to positive and negative frequency solutions of the Dirac equation respectively. Now, the neutrino we will assume to be massless as it is in the Standard Model and to be also a Dirac fermion (as opposed to Majorana fermion). We will also stay away from neutrino flavours for simplicity even though the massless property of neutrinos forbids mixing, which is in turn a slight simplification. Adding a flavour generally requires the mediator to be flavoured as well, which does not necessarily change the general behaviour of the model – it adds an additional complication at both direct and indirect detection.[77] Thus, we can describe the neutrino very similarly to the Dark Matter particle by

$$\mathcal{L}_{\text{neutrino}} = i\bar{\nu}(x)\partial\!\!\!/\,\nu(x);$$

$$\nu(t,\boldsymbol{x}) = \sum_s \int \frac{d^3\boldsymbol{p}}{(2\pi)^3\sqrt{2E_{\boldsymbol{p}}}} \left(b^s_{\boldsymbol{p}}\, u^s(\boldsymbol{p}) e^{-ip\cdot x} + d^{\dagger,s}_{\boldsymbol{p}}\, v^s(\boldsymbol{p}) e^{+ip\cdot x}\right). \tag{6.4}$$

and the respective Dirac conjugate can be constructed as in Eq. (6.2) but is not written explicitly. We now need the final piece of the toy model – the mediator, which mediates the interaction. We choose this mediator to be represented by a complex scalar field. As we did before for Dark Matter and the neutrino, we now write the Lagrangian and the field

$$\mathcal{L}_{\text{mediator}} = \partial_\mu \phi^{0\star} \partial^\mu \phi^0 - M^2 \phi^{0\star}\phi^0\,. \tag{6.5}$$

In this expression M is the mass of the mediator particle and the field is given by the following, similarly to Eq. (4.2).

$$\phi^0(t,\boldsymbol{x}) = \int \frac{d^3\boldsymbol{p}}{(2\pi)^3\sqrt{2E_{\boldsymbol{p}}}} \left(\alpha_{\boldsymbol{p}}\, e^{-ip\cdot x} + \beta^\dagger_{\boldsymbol{p}}\, e^{+ip\cdot x}\right). \tag{6.6}$$

It should be noted that it this toy model we specifically choose a Dirac Dark Matter particle, a complex scalar mediator, and a massless neutrino. A finite combination of fields exists, which will satisfy the Standard Model internal symmetries as we will see and this is only one of them; arguably, it is a bit less mathematically challenging. The purpose of this model is not to describe a complete theory of Dark Matter-neutrino interactions, but to examine the most basic phenomenology and behaviour. In the ideal case, this analysis should provide a relatively strong detection signature which, if detected, will hint at the fact that this model is going in the right direction. Conversely, it could mean that this model is completely irrelevant and there is no chance that Dark Matter can be actually described by a Dirac fermion. Many more possibilities exist and can be explored, even though many of them will give similar behaviour of the model.[75]

6.2 Interaction Mechanism

Now that we have written down the separate components in a way that we can describe them mathematically, it is time to consider the way in which they can interact so that we can see how the different pieces fit together. We have to write an interaction Lagrangian, which includes all three fields. In order for this Lagrangian to be valid, we need to make it abide by the fundamental

internal gauge symmetry of the Standard Model: $U(1) \times SU(2) \times SU(3)$. In particular, we are interested in a exclusively weak interaction and the symmetry governing it will be $U(1) \times SU(2)_L$. In the Standard Model, the neutrino transforms as a lepton doublet $L^\tau = (\nu, l)_L$ under $SU(2)$ transformations. Due to the charged lepton, this doublet brings a conserved charge under $U(1) \times SU(2)$ transformations. Since we want the total charge in the Lagrangian to be zero to satisfy this internal symmetry, we must promote either the Dark Matter field or the Mediator field to a doublet. Promoting the Dark Matter to a doublet is possible and results in a lower bound on the Dark Matter mass of a few GeV.[78,79] What we choose is to promote the mediator to a doublet for slightly simpler considerations by avoiding a two-particle Dark Matter model. This allows us to write the mediator like $\phi^\tau = (\phi^+, \phi^0)$, where now each doublet brings a weak hypercharge and a weak isospin:

$$\begin{aligned} Q_{\nu_L} &= I_{3W} + \frac{Y_W}{2} = \frac{1}{2} + \frac{(-1)}{2} = 0\,, \\ Q_{\ell_L} &= I_{3W} + \frac{Y_W}{2} = -\frac{1}{2} + \frac{(-1)}{2} = -1\,, \\ Q_{\phi^+} &= I_{3W} + \frac{Y_W}{2} = \frac{1}{2} + \frac{1}{2} = 1\,, \\ Q_{\phi^0} &= I_{3W} + \frac{Y_W}{2} = -\frac{1}{2} + \frac{1}{2} = 0\,. \end{aligned} \tag{6.7}$$

Combined, the interaction Lagrangian is now safely invariant under the internal symmetries of the standard model. This allows us to write it like

$$\mathcal{L}_{\text{int.}} = -g\,\bar{\chi} P_L L_j (i\sigma_2)_{jk} \phi_k + \text{h.c.}\,, \tag{6.8}$$

where the j, k indices are contracted and $\sigma_2 = \begin{bmatrix} 0 & -i \\ i & 0 \end{bmatrix}$ is the second Pauli matrix, which ensures correct mixing of the doublets. Additionally, $P_L = \frac{1}{2}(\mathbb{1}_4 - \gamma^5)$ is the left-handed projection operator[b], which ensures the handedness of the neutrino is matched. Finally, g is the coupling strength of the interaction. The Hermitian conjugate is added in the end to ensure $\mathcal{L} \in \mathbb{R}$. Therefore, now we can write the complete Lagrangian of the toy model, which we constructed:

$$\begin{aligned} \mathcal{L} = \underbrace{\bar{\chi}\left(i\partial\!\!\!/ - m\right)\chi + i\bar{\nu}\partial\!\!\!/\,\nu + \partial_\mu \phi^{0\star}\partial^\mu \phi^0 - M^2 \phi^{0\star}\phi^0}_{\text{individual particle terms}} + \\ \underbrace{-g\bar{\chi} P_L \nu \phi^0 - g\bar{\nu} P_R \chi \phi^{0\dagger}}_{\text{neutrino interaction terms}} + \underbrace{g\bar{\chi} P_L\, l\, \phi^+ + g\,\bar{l}\, P_R \chi\, \phi^{+\,\dagger}}_{\text{charged lepton int. terms}}\,. \end{aligned} \tag{6.9}$$

As one can see, this model does not forbid the interaction of Dark Matter with charged leptons, which is not observed in the Universe.[80] This is partially due to the fact that Dirac Dark Matter-charged lepton interactions produce effective electromagnetic coupling.[81] Hence, this interaction channel has to be suppressed in some way and many possibilities exist, both by introducing additional neutrino mixing, but also by introducing neutrino masses.[75,82] In any case, this issue is not discussed in this thesis for dealing with it requires abandoning the simplicity of the model. Additionally, we know that Dark Matter is a stable (or with a long lifetime) particle and therefore between the mediator and the Dark Matter, the Dark Matter particle should be lighter. This prevents spontaneous decay of Dark Matter into the mediator. With these considerations, the model allows for a multitude of interactions involving neutrinos:

[b] $\gamma^5 = i\gamma^0\gamma^1\gamma^2\gamma^3\gamma^4$ is known as the fifth Dirac matrix and it has the anticommutation relation $\{\gamma^5, \gamma^\mu\} = 0$

(1) Dark Matter scatters with a neutrino

(2) Mediator scatters with a neutrino

(3) Dark Matter scatter with a mediator

(4) Dark Matter pair annihilates into neutrino pair

(5) Mediator pair annihilates into neutrino pair

(6) Mediator pair annihilates into Dark Matter pair

(7) Mediator decays into a neutrino and a Dark Matter particle

(8) Inelastic scattering of Dark Matter and mediator into SM particles

We can make the reasonable assumption that the mediator is unstable and does not exist in large quantities in the Universe. Thus, many of the items in the list are not worth examining because they are completely irrelevant – they would occur extremely rarely (if at all) in the cosmos and are thus undetectable anyways. (1) and (4) are of particular interest because they could be involved in significant processes in the present-day and early Universe. (5) could potentially be useful as well for examining the co-annihilation channels for the decoupling of Dark Matter in the early Universe in the scenario where the mediator and Dark Matter masses are similar $M \sim m$,[44] but will not be discussed here.

It is worth mentioning that the scalar mediator could interact with the Higgs boson via a scalar coupling of the form $\mathcal{L}_{\text{scalar}} = \lambda_s H^\dagger H \phi^\dagger \phi$. Here, H is the Higgs doublet and λ_s is the coupling of the scalar interactions. In this thesis, we consider $\lambda_s = 0$ in order to reduce the model parameter space. A study that partly comprise the effect of the Higgs interaction can be found in *Vogl, 2014*[60] and *Garny et al, 2015*[77] .

7 Dark Matter Scattering with Massless Neutrino

In this section we will consider the scattering mechanism $\chi\nu \to \chi\nu$. The goal is to obtain a Lorentz invariant amplitude for the interaction and then use the Golden rule for scattering to compute a differential cross-section, which is then to be integrated to a full cross-section of the interaction. We consider the following components.

- ☐ an in-going neutrino with momentum p_1;
- ☐ an in-going Dark Matter fermion with momentum k_1;
- ☐ an out-going neutrino with momentum p_2;
- ☐ an out-going Dark Matter fermion with momentum k_2.

7.1 Feynman Diagram and Amplitude

Considering the momenta of the particles, the interaction Lagrangian in Eq. (6.9) and the Feynman rules,[73] we can draw the Feynman diagram for the interaction. This is depicted in Figure 7.1.

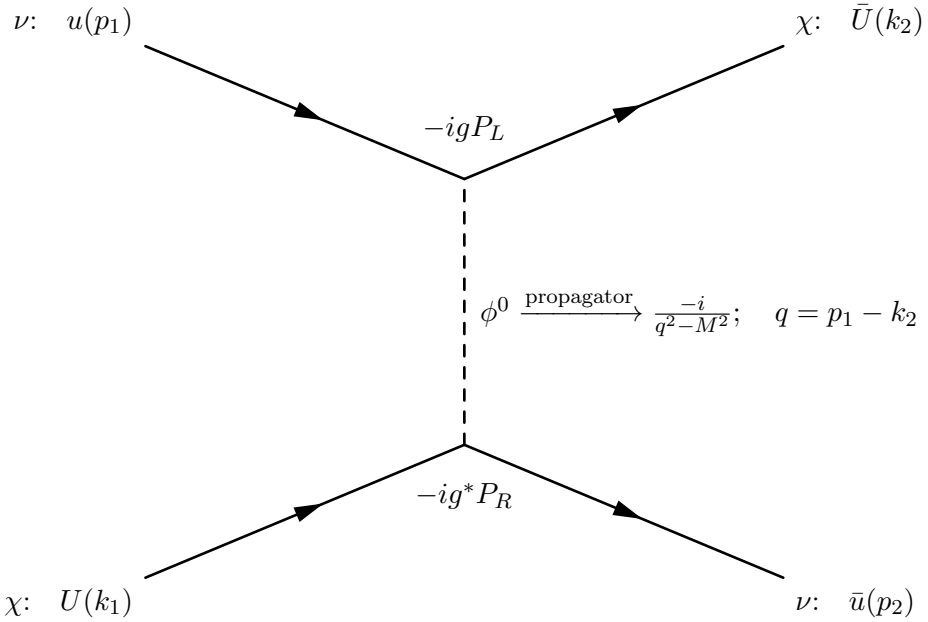

Figure 7.1: Feynman diagram of Dirac DM scattered with a neutrino via a scalar mediator.

Now, using the rules for 'unpacking' a Feynman diagram, we can compute the amplitude of the interaction and write it like

$$\mathcal{M} = |g|^2\, \bar{u}^a(p_2) P_R^{ab} U^b(k_1)\, \frac{i}{q^2 - M^2}\, \bar{U}^c(k_2) P_L^{cd} u^d(p_1)\,, \tag{7.1}$$

where a, b, c, $d = 1, 2, 3, 4$ are the spinorial indices. From now on these index contractions will be implied by square brackets to simplify notation. We can then proceed to find the Hermitian conjugate of the amplitude and noting that

$$(\bar{u}\, P_R\, U)^\dagger = U^\dagger P_R^\dagger (u^\dagger \gamma^0)^\dagger = U^\dagger P_R \gamma^0 u = \bar{U} P_L u\,,$$

we can write

$$\mathcal{M}^\dagger = -i \frac{|g|^2}{q^2 - M^2}\, \left[\bar{u}(p_1) P_R U(k_2)\right]\, \left[\bar{U}(k_1) P_L u(p_2)\right]. \tag{7.2}$$

In the next step we will find the invariant amplitude and average it over all possible spin configurations $\overline{|\mathcal{M}|^2} = \sum_{\text{spins}} \mathcal{M}^\dagger \mathcal{M}$. This is necessary because we are not considering a specific experimental environment with prepared states. Namely, in the Universe all possibilities could exist and should therefore all be considered. The matrix amplitude squared then reads

$$\overline{|\mathcal{M}|^2} = \frac{1}{4} \frac{|g|^4}{(q^2 - M^2)^2} \sum_{s_\nu, s_\chi} \left[\bar{u}(p_1) P_R U(k_2)\right] \left[\bar{U}(k_1) P_L u(p_2)\right]\, \left[\bar{u}(p_2) P_R U(k_1)\right] \left[\bar{U}(k_2) P_L u(p_1)\right].$$

The sum over the outer products can be handled elegantly. It is very handy to now use the relations for the outer products of the spinors, as demonstrated in Eq. (4.14). It should be noted that in the next step, traces start appearing due to contraction of spin indices from different inner products of spinors with helicity operators.

$$
\begin{aligned}
\overline{|\mathcal{M}|^2} &= \frac{|g|^4}{64(q^2-M^2)^2}\,\mathrm{Tr}\left[\not{p}_1(\mathbb{1}+\gamma^5)(\not{k}_2+m)(\mathbb{1}-\gamma^5)\right]\mathrm{Tr}\left[(\not{k}_1+m)(\mathbb{1}-\gamma^5)\not{p}_2(\mathbb{1}+\gamma^5)\right] \\
&= \frac{|g|^4}{64(q^2-M^2)^2}\Big\{\mathrm{Tr}\left[\not{p}_1(\not{k}_2+m)\right] + \cancelto{\text{odd }\gamma^s}{\mathrm{Tr}\left[\not{p}_1\gamma^5(\not{k}_2+m)\right]} + \\
&\qquad\qquad -\cancel{\mathrm{Tr}\left[\not{p}_1(\not{k}_2+m)\gamma^5\right]} - \mathrm{Tr}\left[\not{p}_1\gamma^5(\not{k}_2+m)\gamma^5\right]\Big\} \\
&\times\Big\{\mathrm{Tr}\left[(\not{k}_1+m)\not{p}_2\right] - \cancel{\mathrm{Tr}\left[(\not{k}_1+m)\gamma^5\not{p}_2\right]} + \cancel{\mathrm{Tr}\left[(\not{k}_1+m)\not{p}_2\gamma^5\right]} - \mathrm{Tr}\left[(\not{k}_1+m)\gamma^5\not{p}_2\gamma^5\right]\Big\} \\
&= \frac{|g|^4}{64(q^2-M^2)^2}\left\{2\mathrm{Tr}\left[\not{p}_1\not{k}_2\right]\right\}\left\{2\mathrm{Tr}\left[\not{k}_1\not{p}_2\right]\right\} = \frac{|g|^4}{((p_1-k_2)^2-M^2)^2}(p_1\cdot k_2)(k_1\cdot p_2),
\end{aligned}
$$

where all traces of a product of odd number of gamma matrices vanish.[73] So far, we only considered neutrino scattering with Dark Matter. Now, we will add also Dark Matter scattering with an anti-neutrino. Even though the amplitude is not the exact same, the computation of the averaged invariant amplitude gives an identical result. Summing the two probabilities, we obtain a final expression for the Feynman invariant amplitude

$$
\overline{|\mathcal{M}|^2} = \frac{2|g|^4}{((p_1-k_2)^2-M^2)^2}(p_1\cdot k_2)(k_1\cdot p_2)\,. \tag{7.3}
$$

7.2 Elastic Scattering Cross-section

Now that we know the amplitude of the interaction, we can move on and find the cross-section and analyse it. Conservation of energy implies $E_{p1}+E_{k1}=E_{p2}+E_{k2}$. This can be summarised to conservation of 4-momentum. Additionally, here we consider a massless neutrino (or simply UR $p_\nu \gg m_\nu$), so then $E_{p_i}=|\boldsymbol{p}_i|$. We proceed to consider the most general possible frame in which the interaction takes place. Without loss of generality, we can align the z-axis with the axis of movement of the incident DM particle ($\boldsymbol{k}_1=|\boldsymbol{k}_1|\hat{z}$). Therefore,

$$
\begin{aligned}
k_1^\mu &= E_{k1}(1,0,0,\beta) \\
p_1^\mu &= E_{p1}(1,\sin\theta\cos\phi,\sin\theta\sin\phi,\cos\theta) \\
p_2^\mu &= E_{p2}(1,\sin\theta'\cos\phi',\sin\theta'\sin\phi',\cos\theta') \\
k_2^\mu &= k_1^\mu + p_1^\mu - p_2^\mu,
\end{aligned} \tag{7.4}
$$

where the angles θ and ϕ are standard angles in spherical coordinates denoting the relative incidence of the incoming neutrino $\nu(p_1)$ with respect to the incoming Dark Matter particle $\chi(k_1)$. Similarly, θ' and ϕ' are angles at which the outgoing neutrino $\nu(p_2)$ is scattered. Finally, $\beta=\frac{|\boldsymbol{k}_1|}{E_{k1}}$. And so, the scalar product in Eq. (7.3) can be simplified as follows

$$
\begin{aligned}
k_1\cdot p_2 &= E_{k1}E_{p2}(1-\beta\cos\theta') \\
p_1\cdot k_2 &= p_1\cdot k_1 + p_1^2 - p_1\cdot p_2 = \\
&= E_{p1}E_{k1}(1-\beta\cos\theta) - E_{p1}E_{p2}\underbrace{(1-\sin\theta\sin\theta'\underbrace{(\cos\phi\cos\phi'+\sin\phi\sin\phi')}_{\cos(\phi-\phi')}-\cos\theta\cos\theta')}_{\Delta}.
\end{aligned}
$$

We use the notation from Ref.[75] and define $\mu = \cos\theta$ and from there we can also define the angle-dependent variable $\Delta = \mu\mu' + \sqrt{1-\mu^2}\sqrt{1-\mu'^2}\cos(\phi-\phi')$. If we now consider the Mandelstam variables

$$\begin{aligned} s &= (k_1+p_1)^2 = E_{k1}^2 + E_{p1}^2 + 2E_{k1}E_{p1} - E_{p1}^2\sin^2\theta - E_{p1}^2\cos^2\theta - E_{k1}^2\beta^2 - 2E_{p1}E_{k1}\beta\cos\theta \\ &= \underbrace{E_{k1}^2(1-\beta^2)}_{m^2} + 2E_{p1}E_{k1}(1-\beta\mu) \end{aligned}$$

and similarly for the other two variables (7.5)

$$u = (p_1-k_2)^2 = (p_2-k_1)^2 = m^2 - 2E_{k1}E_{p2}(1-\beta\mu')$$

$$t = (p_1-p_2)^2 = -2E_{p1}E_{p2}(1-\Delta), \tag{7.6}$$

an easy substitution can be made for a transition towards Mandelstam variables.

$$k_1\cdot p_2 = \frac{m^2-u}{2} \qquad \text{and} \qquad p_1\cdot k_2 = \frac{s+t-m^2}{2}$$

$$\implies \qquad |\mathcal{M}|^2 = \frac{|g|^4}{2(u-M^2)^2}(s+t-m^2)(m^2-u)$$

If we now eliminate one of these variables by using the standard property of Mandelstam variables $s+t+u = \Sigma_i m_i^2 = 2m^2$, we get

$$|\mathcal{M}(u)|^2 = \frac{|g|^4}{2}\left(\frac{u-m^2}{u-M^2}\right)^2 . \tag{7.7}$$

Obtaining a differential cross-section expression

In the most general form, as derived in Eq.(4.11), the *Golden rule* for a scattering cross-section of this interaction can be written as

$$d\sigma_{\text{sc.}} = |\mathcal{M}|^2 \frac{\delta^4(p_1+k_1-p_2-k_2)\, d^3\boldsymbol{p}_2 d^3\boldsymbol{k}_2}{64\pi^2 E_{p2}E_{k2}\underbrace{\sqrt{(p_1\cdot k_1)^2 - m^2m_\nu^2}}_{\xi}} . \tag{7.8}$$

Written in this way, it can be easily seen that $\xi = (p_1\cdot k_1) = \frac{s-m^2}{2}$, but also, it can be written as $\xi = |\boldsymbol{p}_1|E_t$, where $E_t = E_{p1}+E_{k1} = E_{p2}+E_{k2}$ is the total energy and is kept constant. We will now switch to a centre-of-momentum frame to simplify calculation. This, of course, would limit our result, but as we will see in the final expression, we will have only Lorentz invariant variables, which would suggest that the differential cross-section is frame-independent as it should be. Integrating over $\boldsymbol{k}_2$ is trivial as if we write $\boldsymbol{p}_2 = -\boldsymbol{k}_2$ and make E_{k2} independent of $\boldsymbol{k}_2$, we are left with integration of a 3-dimensional delta function, which gives simply identity:

$$d\sigma_{\text{sc.}} = |\mathcal{M}|^2 \frac{\delta(E_{p1}+E_{k1}-E_{p2}-E_{k2})\, d^3\boldsymbol{p}_2}{64\pi^2\, .E_{p2}E_{k2}\,\xi}$$

If we take a look at the infinitesimal volume $d^3\boldsymbol{p}_2$ in momentum space, we can rewrite it in terms of the absolute momentum and an infinitesimal solid angle $d\Omega$ such that $d^3\boldsymbol{p}_2 = |\boldsymbol{p}_2|^2\, d|\boldsymbol{p}_2|d\Omega$. Before integrating over $|\boldsymbol{p}_2|$, we must first look at the delta function as it is dependent on our variable of interest:

$$\delta[f(|\boldsymbol{p}_2|)] = \delta[E_t - |\boldsymbol{p}_2| - \sqrt{|\boldsymbol{p}_2|^2+m^2}] = \frac{\delta[|\boldsymbol{p}_2|-|\boldsymbol{p}_2^0|]}{|f'(|\boldsymbol{p}_2|)|_{|\boldsymbol{p}_2|=|\boldsymbol{p}_2^0|}} = -\frac{E_{k2}\,\delta[|\boldsymbol{p}_2|-|\boldsymbol{p}_2^0|]}{\underbrace{(|\boldsymbol{p}_2|+E_{k2})}_{E_t}},$$

where $|\boldsymbol{p}_2^0|$ is the actual momentum of the outgoing neutrino and we can put it back to $|\boldsymbol{p}_2| = E_{p2}$ for simplicity. Hence,

$$d\sigma_{\text{sc.}} = -|\mathcal{M}|^2 \frac{E_{p2}\, d\Omega}{64\pi^2 E_t\, \xi}.$$

It would be intuitive to define the solid angle in terms of the already defined (in the incoming DM frame) angles such that $d\Omega = \sin\theta'\, d\theta' d\phi'$, but that complicates the derivation so we will express it in terms of the angle α between $\boldsymbol{p}_1$ and $\boldsymbol{p}_2$ and their azimuth β so that $d\Omega = \sin\alpha\, d\alpha\, d\beta$. If we take a look at the Mandelstam variable t, we can perform a substitution:

$$t = (p_1 - p_2)^2 = 2|\boldsymbol{p}_1||\boldsymbol{p}_2|(\cos\alpha - 1) \quad \Longrightarrow \quad dt = -2|\boldsymbol{p}_1||\boldsymbol{p}_2|\sin\alpha\, d\alpha$$
$$\Longrightarrow\ d\sigma_{\text{sc.}} = |\mathcal{M}|^2 \frac{dt}{64\pi|\boldsymbol{p}_1|E_t\,\xi}\frac{d\beta}{2\pi} = |\mathcal{M}|^2 \frac{dt}{64\pi\xi^2},$$

assuming that the differential cross-section is independent of the azimuth. We can now perform one last substitution $t \to u$ and express ξ in terms of s. The desired result follows and is indeed Lorentz invariant

$$\frac{d\sigma_{\text{sc.}}}{du} = \frac{-|\mathcal{M}(u)|^2}{16\pi(s-m^2)^2}\,. \tag{7.9}$$

It agrees with Eq. (B5) of *Del Campo, 2017*.[75] For simplicity of computation, we further use the change of variables

$$w = 1 - \frac{u}{m^2}\,, \quad dw = -\frac{du}{m^2}\,; \quad y = \frac{s-m^2}{m^2} = \frac{2E_{p1}E_{k1}}{m^2}(1-\beta\cos\theta)\,, \tag{7.10}$$

and then express the differential cross-section as

$$\frac{d\sigma_{\text{sc.}}}{du} = -\frac{|\mathcal{M}(u)|^2}{16\pi(s-m^2)^2} \Rightarrow \frac{d\sigma_{\text{sc.}}}{dw} = \frac{g^4}{32\pi}\frac{m^2}{y^2}\frac{w^2}{(m^2 - m^2 w - M^2)^2}\,. \tag{7.11}$$

We are now fully set up to obtain the full cross-section by integrating over the newly defined w. However, this task is not as easy as it might seem because the integration boundaries have to be selected very carefully.

Integration boundaries

In order to obtain a cross-section, we must integrate over all possible outcomes in the parameter space. Since the Feynman invariant amplitude is expressed in terms of the invariant u, it suffices to integrate (7.11) over all possible values of w, which are determined by the physically allowed values of the Mandelstam variables for the given configuration.

Locality condition

Due to locality of a momentum-product vector, in general, it is required that,[83][84]

$$stu \geq as + bt + cu, \tag{7.12}$$

where $a, b, c \in \mathbb{R}$ are constants, that depend solely on the mass of the scattered particles. For the specific masses of this problem, we have that $a = c = 0$ and $b = m^4$. Hence,

$$t(su - m^4) \geq 0$$
$$\Longrightarrow \quad \text{I:}\ \ t \geq 0 \ \text{ and } \ su \geq 0 \qquad \text{OR} \qquad \text{II:}\ \ t \leq 0 \ \text{ and } \ su \leq m^4\,.$$

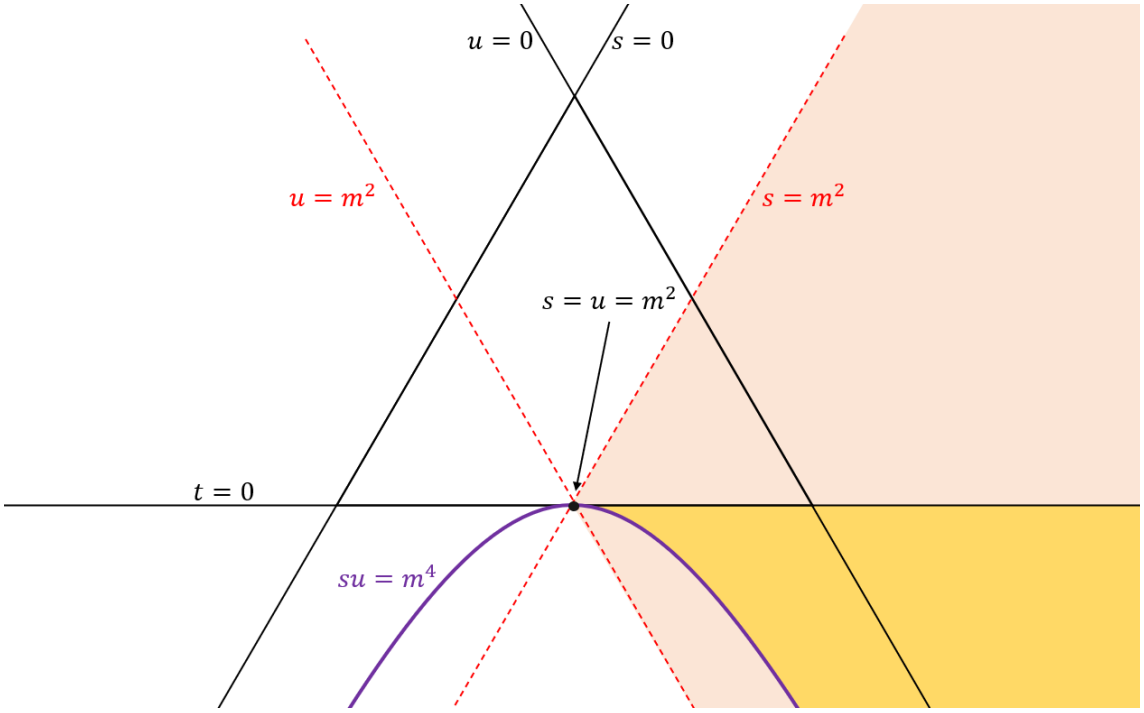

Figure 7.2: Mandelstam plane for Dirac DM and massless neutrino: Variables grow positive towards the centre of the triangle. Only the region shaded in yellow is physically admissible. Light-red region denotes $\{u < m^2\} \cap \{s > m^2\}$.

4-vector condition

In general for any 4-momentum vectors p_a and p_b it holds that $p_a p_b \geq m_a m_b$ but also $(p_a + p_b)^2 \geq (m_a + m_b)^2$ and $(p_a - p_b)^2 \leq (m_a - m_b)^2$. In our u-channel, this translates to

$$t \leq 0; \qquad s \geq m^2; \qquad u \leq m^2 \,.$$

These can also be deduced from eq. (7.5). Therefore, case II of the locality condition holds and $su \leq m^4$. We can now start cutting into the Mandelstam plane (Fig. 7.2).

Final boundaries

$t \leq 0$ requires that we stay down from the $t = 0$ line. In terms of the newly defined variable w, this translates to

$$t \leq 0 \quad \Longleftrightarrow \quad u + s \geq 2m^2 \quad \Longleftrightarrow \quad m^2(y + 1 + 1 - w) \geq 2m^2 \quad \Longrightarrow \quad \boxed{w \leq y} \,.$$

$u \leq m^2$ and $s \geq m^2$ require that we stay in the light-red region of Figure 7.2, right of the two dashed red lines. The final condition is that $su \leq m^4$. $su = m^4$ defines a hyperbola in the Mandelstam plane and the condition requires us to stay above it. Combined with $t \leq 0$, it turns out that these two conditions are stronger than $u \leq m^2$ and $s \geq m^2$, and define the 'allowed'

yellow region in Figure 7.2. [c] In terms of w, this translates to

$$su \leq m^4 \quad \Longleftrightarrow \quad (y+1)(1-w) \leq 1 \quad \Longleftrightarrow \quad w(y+1) \geq y\,.$$

This allows for two different situations – positive or negative $(y+1)$. However, we have already cut the Mandelstam plane in a way that excludes the region where $y < -1$ (corresponding to $s < 0$). Therefore, we should only consider the case where $y > -1$ and so $\boxed{w \geq \frac{y}{y+1}}$. Finally, we reach the complete boundaries of integration: $\frac{y}{y+1} \leq w \leq y$. Following this independent derivation, the result agrees with the boundaries given in *Del Campo, 2017*.[75]

Integration

Integration with the specified boundaries $\int_{\frac{y}{y+1}}^{y} \frac{d\sigma_{\text{sc.}}}{dw} dw$ gives

$$\sigma_{\text{sc.}} = \frac{|g|^4}{32\pi m^4 y^2}\left\{\frac{m^2y^2}{y+1} - \frac{(m^2-M^2)^2}{M^2+m^2(y-1)} - \frac{(y+1)(m^2-M^2)^2}{m^2-M^2(y+1)} \quad + \right.$$
$$\left. + \quad 2(m^2-M^2)\ln\left[1+\frac{m^2y^2}{M^2(y+1)-m^2}\right]\right\}. \tag{7.13}$$

Unit conversion

The computation so far has been done in the standard for QFT notation where $\hbar = c = 1$. However, now we want to measure the cross-section in SI units of cm^2 and to input masses and energies in units of eV. Therefore, the cross-section should be written as

$$\sigma_{\text{sc.}}[\text{cm}^2] = 10^4\,\frac{\hbar^2c^2}{e^2} \times \sigma_{\text{sc.}}\left[\frac{1}{\text{kg}^2}\right],$$

where $\hbar$, c, and e are Planck's constant, the speed of light in vacuum, and the elementary charge respectively. This is done by simple dimensional analysis.

Limiting cases and asymptotic behaviour

Since the weakly interacting massive DM particle (WIMP) belongs to a category of DM models known as *cold* DM, we can assume low velocities on average and hence also low 3-momentum. This effect is especially true when the DM is compared to the ultra-relativistic neutrino. Hence, it should be mostly the energy of the incoming neutrino that is varied as neutrinos of a wide range of energies can be found in the cosmos. The point of comparison is the DM mass so that in the low/high E_{p1} limit we have $E_{p1} \ll m$ and $E_{p1} \gg m$ respectively. In the input parameter y of equation (7.13), this translates to $y \ll 1$ and $y \gg 1$. In order to obtain simplified expressions in those two limiting cases, we can take power series expansion in y or $\frac{1}{y}$.

- ☐ Low-E_{p1} limit: $\sigma_{\text{sc.}} \approx \frac{g^4m^2y^2}{32\pi(m^2-M^2)^2} + \frac{g^4m^2M^2y^2}{16\pi(m^2-M^2)^3} + \mathcal{O}(y^4)$
- ☐ High-E_{p1} limit: $\sigma_{\text{sc.}} \approx \frac{g^4}{32\pi m^2 y} + \mathcal{O}(\frac{1}{y^2})$

[c] Writing down the intersections of $u = m^2$ and $su = m^4$ gives only one solution ($s = u = m^2$). Thus, the red dashed line does not intersect the purple line $\forall t < 0$ and the yellow region remains uncut further.

As for the asymptotic or ill-defined behaviour, one can see that there are 4 possible causes – one for each term in eq. (7.13). The first three have to do with values where the denominator goes to zero and the term explodes and the fourth has to do with the undefined region of the logarithm. We can eliminate most of them by considering only the region of the parameter space where $y > 0$ (by definition) and $M > m$ (by stability of DM).

The **first term** in Eq. (7.13) is $\frac{m^2y^2}{y+1}$ and one can easily see that for positive y it has no asymptotes.

The **second term** is $\frac{(m^2-M^2)^2}{M^2+m^2(y-1)}$. The term blows up when

$$m^2(y-1)+M^2=0 \quad \Longrightarrow \quad y=1-\frac{M^2}{m^2}. \quad \text{But we have } y>0 \text{ so for}$$

$$\text{this asymptote to be accessible, we must have } 1-\frac{M^2}{m^2}>0 \quad \Longleftrightarrow \quad M^2<m^2.$$

This is not allowed with the current restriction on the parameter space. Therefore, the asymptote is inaccessible.

The **third term** is $\frac{(y+1)(m^2-M^2)^2}{m^2-M^2(y+1)}$ and similarly to the second term, it blows up when

$$m^2-M^2(y+1)=0 \quad \Longrightarrow \quad y=\frac{m^2}{M^2}-1. \quad \text{Again, } y>0 \text{ so for}$$

$$\text{the asymptote to be accessible, we must have } \frac{m^2}{M^2}-1>0 \quad \Longleftrightarrow \quad M^2<m^2.$$

For the same reason as the second term, the third term is also inaccessible.

The **log term** is $2(m^2-M^2)\ln\left(1+\frac{m^2y^2}{M^2(y+1)-m^2}\right)$. It cannot blow up to infinity for the same reasons as the third term since the argument in the log has the same denominator. However, one should also examine the region of the parameter space where the logarithm is undefined i.e. argument lies on the real non-positive axis. Hence, the logarithm is undefined when

$$\frac{A(M,m,y)}{B(M,m,y)}=\frac{M^2+M^2y-m^2+m^2y^2}{M^2(y+1)-m^2}<0 \quad \Longrightarrow \quad \begin{vmatrix} A>0 \\ B<0 \end{vmatrix} \quad \text{or} \quad \begin{vmatrix} A<0 \\ B>0 \end{vmatrix}$$

By looking at the mathematics for the third term, where $B(M,m,y)$ is also found, one can conclude that for $y>0$ and $M>m$, $B(M,m,y)>0$. Therefore, the logarithm is undefined when

$$\begin{aligned} A(M,m,y) &= M^2+M^2y-m^2+m^2y^2 \\ &= m^2\left(\underbrace{y+\frac{M^2+|M^2-2m^2|}{2m^2}}_{>0\,\forall\,M,m,y>0}\right)\left(\underbrace{y+\frac{M^2-|M^2-2m^2|}{2m^2}}_{\text{must be negative}}\right)<0 \end{aligned} \tag{7.14}$$

Since the second term has to be negative for the inequality to hold, it introduces an upper boundary for the region in y where the logarithm is undefined ($y<\frac{-M^2+|M^2-2m^2|}{2m^2}$). Now the question is whether this upper boundary lies before or after the zero in y. Hence, we must examine $|M^2-2m^2| \lessgtr M^2$. It turns out that for positive m and M and for $M>m$, it holds that $|M^2-2m^2|<M^2$ and so region where the logarithm is undefined lies completely in $y<0$. Therefore, for $y>0$ and $M>m$, the logarithm is defined everywhere.

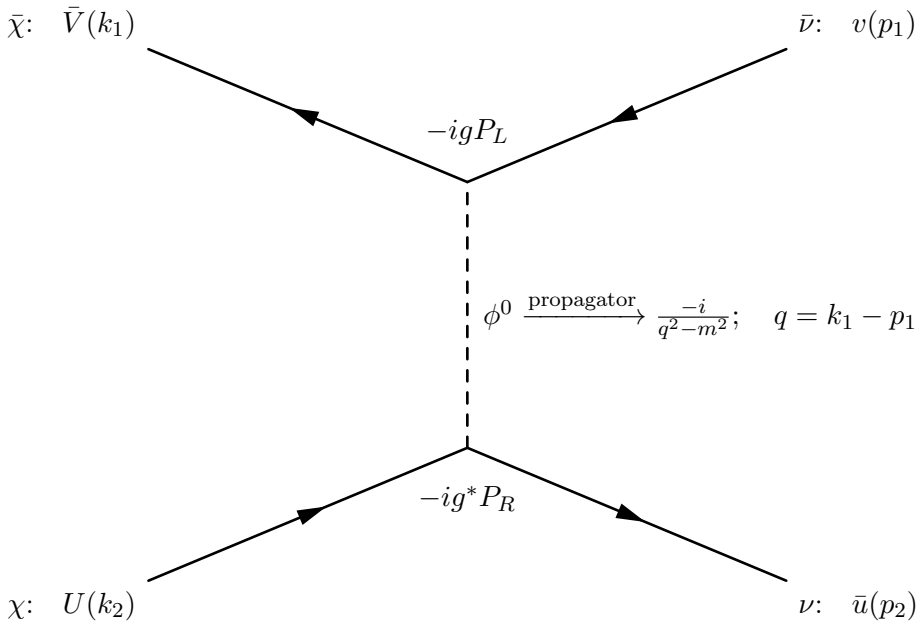

Figure 8.1: Feynman diagram of Dirac DM annihilated into a neutrino and anti-neutrino via a scalar mediator

An interesting limit to consider is the limit where the log term vanishes naturally from equation (7.13). This happens when its argument is identity (i.e. $\frac{m^2y^2}{M^2(1+y)-m^2} \approx 0$) and could simplify the expression and its computation greatly. This limit is reached either when $y \ll 1$ or when $m \ll M$.

8 Dark Matter Annihilation to Neutrinos

If we consider the full elastic scattering cross-section as in Eq. (7.13), we notice that despite being well-defined and well-behaving, it is an intimidating function with quite a few independent parameters. After making a smart approximation, which revolves around the idea that Dark Matter is cold-ish, we can reduce the system's parameter space. It comes from $y = \frac{2E_{p1}E_{k1}}{m^2}(1 - \beta\cos\theta) \approx \frac{2E_{p1}}{m}$, which eliminates the θ-dependence and the dependence on Dark Matter momentum. This is equivalent to saying that the Dark Matter particle is stationary at interaction, which would not be far from the truth, considering the ultra-relativistic nature of the neutrino. In this section and the following chapter, we aim to reduce the parameters to 3 by imposing an additional condition – the correct abundance of Dark Matter in the Universe. Here, we begin by examining in detail the Dark Matter self-annihilation, which governs the decoupling in the early Universe, which in turn governs the abundance as discussed in Chapter I.

8.1 Feynman Diagram and Amplitude

By the same interaction Lagrangian (6.9), one can also consider an interaction $\chi\bar{\chi} \to \nu\bar{\nu}$ where DM annihilates into neutrinos. The Feynman diagram of this interaction is presented in Figure 8.1.

Variable	Definition	Full expression	Approx. in v up to $\mathcal{O}(v^4)$
s	$(k_1+k_2)^2$	$4E_k^2$	$4m^2+4m^2v^2$
t	$(k_1-p_1)^2$	$2E_k\lvert\boldsymbol{k}_1\rvert\cos\theta - E_k^2 - \lvert\boldsymbol{k}_1\rvert^2$	$-m^2+2m^2\cos\theta v - 2m^2v^2 + 2m^2\cos\theta v^3$
u	$(k_1-p_2)^2$	$-2E_k\lvert\boldsymbol{k}_1\rvert\cos\theta - E_k^2 - \lvert\boldsymbol{k}_1\rvert^2$	$-m^2-2m^2\cos\theta v - 2m^2v^2 - 2m^2\cos\theta v^3$

Table 8.1: Mandelstam variables for DM annihilation into neutrinos. Approximation is made by expanding in power series around $v=0$.

Therefore, the Feynman invariant amplitude can be written like

$$\begin{aligned}\mathcal{M} &= i\left[\bar{u}(p_2)\,P_R\,U(k_2)\right]\frac{g^2}{q^2-M^2}\left[\bar{V}(k_1)\,P_L\,v(p_1)\right]\\ \mathcal{M}^\dagger &= -i\left[\bar{v}(p_1)\,P_R\,V(k_1)\right]\frac{g^2}{q^2-M^2}\left[\bar{U}(k_2)\,P_L\,u(p_2)\right],\end{aligned}\tag{8.1}$$

and therefore, summing over final spin configurations and averaging over initial spins gives

$$\begin{aligned}\overline{|\mathcal{M}|^2} &= \frac{1}{4}\sum_{s_\nu,\,s_\chi}\mathcal{M}^\dagger\,\mathcal{M}\\ &= \frac{|g|^4}{64(q^2-M^2)^2}\,\mathrm{Tr}\left[\not{p}_1(\mathbb{1}+\gamma^5)(\not{k}_1-m)(\mathbb{1}-\gamma^5)\right]\mathrm{Tr}\left[(\not{k}_2+m)(\mathbb{1}-\gamma^5)\not{p}_2(\mathbb{1}+\gamma^5)\right]\\ &= \frac{g^4}{((k_1-p_1)^2-M^2)^2}\,(k_2\cdot p_2)\,(p_1\cdot k_1),\end{aligned}\tag{8.2}$$

similarly to the calculation for scattering presented in the previous question. From now on the calculations will be made in the centre-of-momentum frame s.t. $\boldsymbol{k}_1=-\boldsymbol{k}_2$ and $\boldsymbol{p}_1=-\boldsymbol{p}_2$ and all energies of the particles are equal. This makes most sense so that one can easily obtain an expression for the relative velocity of the incoming DM particles. If the DM particles initially travel on the z-axis, then the polar angle θ can be the angle at which the anti-neutrino is emitted. The Mandelstam variables in this frame can be found in Table 8.1.

We can now rewrite the amplitude by substituting the 4-vector invariant products with Mandelstam variables:

$$(p_1\cdot k_1)=(p_2\cdot k_2)=E_k^2-E_k|\boldsymbol{k}_1|\cos\theta=\frac{m^2-t}{2}\quad\Longrightarrow\quad|\mathcal{M}|^2=\frac{g^4}{4}\left(\frac{t-m^2}{t-M^2}\right)^2\tag{8.3}$$

8.2 Annihilation Cross-section

Again, we start from a general expression for a reaction of the kind $1+2\to3+4$:

$$d\sigma_A=|\mathcal{M}|^2\frac{\delta^4(k_1+k_2-p_1-p_2)\;d^3\boldsymbol{p}_1 d^3\boldsymbol{p}_2}{64\pi^2E_{p1}E_{p2}\underbrace{\sqrt{(k_1\cdot k_2)^2-m^4}}_{2E_k|\boldsymbol{k}_1|}}\tag{8.4}$$

Similarly to what is done above, we proceed to integrate over $d^3\boldsymbol{p}_1$ without problems, then obtain a factor of $\frac{1}{2}$ when reworking the delta function to integrate over $d|\boldsymbol{p}_2|$. Keeping in mind that

all energies are equal gives the differential cross-section:

$$d\sigma_A = |\mathcal{M}|^2 \frac{|\boldsymbol{p}_1|^2}{64\pi E_{p1} E_{p2} E_k |\boldsymbol{k}_1|} \frac{d\Omega}{4\pi} = |\mathcal{M}|^2 \frac{1}{64\pi E_k |\boldsymbol{k}_1|} \frac{d\Omega}{4\pi} = |\mathcal{M}|^2 \frac{1}{16\pi s} \frac{E_k}{|\boldsymbol{k}_1|} \frac{d\Omega}{4\pi}$$

We can now write [d] $\frac{|\boldsymbol{k}_1|}{E_k} = v = \frac{v_r}{2}$, where v_r is the relative velocity between the DM particles. This gives a general frame-independent expression:

$$d\sigma_A \, v_r = |\mathcal{M}|^2 \frac{1}{16\pi s} \frac{d\Omega}{4\pi} \tag{8.5}$$

We can then move on to rewriting the last line in terms of v and then proceed to expand in the non-relativistic limit $v \ll 1$. Doing so (intermediate expression in appendix) and then integrating the expression over the solid angle gives

$$\begin{aligned} d\sigma_A \, v_r &= g^4 \frac{\left(-2m^2(1+v^2) + 2m^2 v (1+v^2)\cos\theta\right)^2}{256\,\pi\, m^2 (1+v^2)\left(-(m^2+M^2) - 2m^2v^2 - 2m^2 v(1+v^2)\cos\theta\right)^2} \frac{\sin\theta\, d\theta\, d\phi}{4\pi} \\ \implies \sigma_A \, v_r &= \underbrace{g^4 \frac{m^2}{64\,\pi (m^2+M^2)^2}}_{a \in \mathbb{R}_{++}} + \underbrace{g^4 \frac{-m^6 - 3\,m^4 M^2 + m^2 M^4}{48\,\pi (m^2+M^2)^4}}_{b \in \mathbb{R}} v^2 + \\ &\quad + \underbrace{g^4 \frac{49\,m^{10} + 140\,m^8 M^2 + 186\,m^6 M^4 - 140\,m^4 M^6 + 5\,m^2 M^8}{960\,\pi (m^2+M^2)^6}}_{d \in \mathbb{R}_{++}} v^4 + \mathcal{O}(v^6) \end{aligned} \tag{8.6}$$

Taking the thermal average for $\sigma_A \, v_r$ at the time of the freeze-out gives $\langle \sigma_A \, v_r \rangle = a + \frac{9}{4} b v^2 + \frac{135}{32} d v^4$, which is now to be compared to the value that gives the correct thermal relic abundance. That is $\langle \sigma_A \, v_r \rangle \approx 3 \times 10^{-26} \frac{\text{cm}^3}{\text{s}}$, $\langle \sigma_A \, v_r \rangle \approx 6 \times 10^{-26} \frac{\text{cm}^3}{\text{s}}$, or $\langle \sigma_A \, v_r \rangle \approx 9 \times 10^{-26} \frac{\text{cm}^3}{\text{s}}$ for a constant, v^2 -dependent, and v^4-dependent $\sigma_A \, v_r$ respectively.[85] With this, the mathematical development of the model ends. We have now arrived at a place where we have an approximate mathematical expression of a measured observable. The exact substitution and further development are left for the following chapter.

9 Co-annihilation Channels

The model, as governed by the Lagrangian in Eq. (6.9), introduces two new 'dark' particles – a mediator and a Dark Matter particle. As discussed already, the Dark Matter particle has to be (nearly) stable and this is why by imposing the condition $M > m$: we forbid Dark Matter decay being the lightest particle of the new physics content. On the contrary, the mediator can decay, and the decay channel is $\phi \to \chi\nu$. In the limit of $M \gg m$, the mediator decouples from the thermal bath a lot earlier than Dark Matter. Even if there was some significant number density of the mediator, after decoupling it quickly decayed into Dark Matter, thus injecting more particles in the Dark Matter population (assumed to be in thermal and kinetic equilibrium). In this way, the mediator abundance is negligible at Dark Matter decoupling and it plays no significant role. However, in the limit of $M \sim m$, the two particles decouple almost simultaneously. Even though, again, after decoupling the mediator would decay to Dark Matter, the presence of another dark

[d] Expanding in m and v gives $\frac{|\boldsymbol{k}_1|}{E_k} = \frac{mv}{\sqrt{1-v^2}} \frac{1}{\sqrt{\frac{m^2 v^2}{1-v^2} + m^2}} = v$

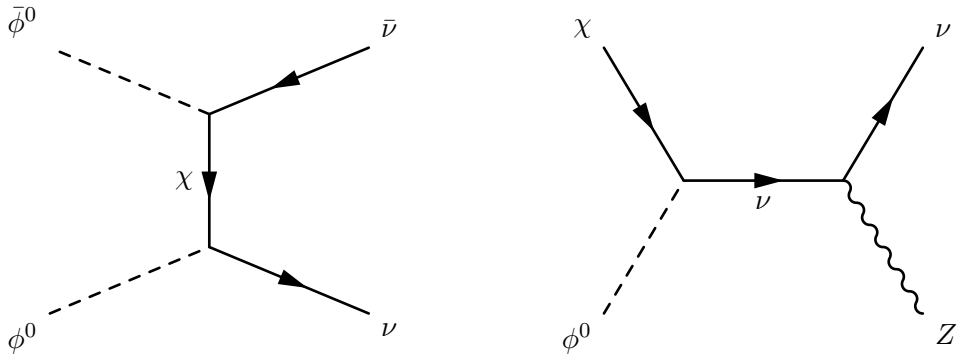

Figure 9.1: Feynman diagrams of two interactions, which could take place at Dark Matter decoupling and must be considered in the mass degenerate limit. On the left, a mediator pair annihilates into neutrinos. On the right, Dark Matter and a mediator co-annihilate into Standard Model particles

particle with large energy density at decoupling requires the consideration of additional annihilation and co-annihilation channels.[86] These can be quite complicated to compute and account for many more interactions that must be considered. Two of these interactions are represented in Figure 9.1, which showcases the most basic (co-)annihilation interactions[e]. These two and any additional interactions come with their own definitive properties and interaction strengths, thus providing new annihilation cross-sections, which must be accounted for. Mathematically and more in general, the *effective* annihilation cross-section can be written like

$$\sigma_{\text{eff}} v = \sum_{i,j} \frac{n_i n_j}{(\Sigma_k n_k)^2} \sigma_{ij} v \,, \tag{9.1}$$

where the number densities n are taken at equilibrium and the summation is over all relevant (co-)annihilation interactions that participate in the freeze-out.[60] The relative particle velocity v can be considered to be the same for all interactions as the Dark Matter and the mediator are very similar in mass and in kinetic equilibrium at decoupling. As the number densities of non-relativistic objects in equilibrium with a thermal bath are related to the masses, and the temperature at decoupling by a Boltzmann distribution like $n_i \propto (m_i T)^{3/2} \exp(-m_i/T)$, in the mass-degenerate limit, one can expand Eq. (9.1) so that the effective cross-section is of the form

$$\sigma_{\text{eff}} v = \sigma_A v + \sigma_{\chi\phi} v \, e^{-\frac{M-m}{T}} + \sigma_{\phi\phi} v \, e^{-2\frac{M-m}{T}} \,, \tag{9.2}$$

where $\sigma_A v$ is the already computed Dark Matter self-annihilation cross-section as in Eq. (8.6). The following two terms correspond to co-annihilation and mediator self-annihilation cross-sections respectively. The latter two are strongly suppressed in the non-degenerate-in-mass limit $M - m \gg T$ by exponential factors but become relevant and thermally accessible once $M - m \lesssim T$. As will be discussed more in Section 11.2, there is a rough lower limit on the temperature of decoupling of Dark Matter of around $T \gtrsim \mathcal{O}(\text{MeV})$, and therefore, the co-annihilations should be considered only for dark particle mass differences on and below the MeV scale.

This subtopic, however, is not studied in detail in this thesis and the following discussion is only meant to demonstrate superficially how the problem could be approached. The Dark Matter annihilation cross-section as in Eq. (8.6) can be expressed for simplicity as $\sigma_A v = \frac{g^4}{m^2} C_{\chi\chi}$, where

[e] It should be noted that mediator annihilations into Dark Matter are irrelevant as they do not change the total number density of dark particles.

$C_{\chi\chi}$ is a dimensionless constant, which depends solely on mass and temperature ratios. Even though the full computation for co-annihilation and mediator annihilation are not performed, one can expect that they can be written in a similar form. If f is a parameter representing the coupling strength to weak gauge bosons, then any co-annihilation will have one vertex corresponding to DM-neutrino coupling and one corresponding to gauge coupling (See right side of Fig. 9.1). Therefore, the co-annihilation cross-section can be written like $\sigma_{\chi\phi}v = \frac{g^2 f^2}{m^2} C_{\chi\phi}$ and the C constant now also accommodates the exponential factors. In parallel to *Vogl, 2014*,[60] which treats DM-quark coupling, for mediator annihilation one can expect a single diagram with two DM-neutrino coupling vertices and plenty of diagrams with two gauge coupling vertices. Thus, the dominant term in the mediator annihilation cross-section will be a f^4 term and the cross-section could be written like $\sigma_{\phi\phi}v \approx \frac{f^4}{m^2} C_{\phi\phi}$. Therefore, for the energy density of Dark Matter in the Universe, we can write

$$\Omega_{\mathrm{DM}}\, h^2 \sim \frac{1}{\langle \sigma_{\mathrm{eff}} v \rangle} \approx \frac{m^2}{g^4 \langle C_{\chi\chi} \rangle + g^2 f^2 \langle C_{\chi\phi} \rangle + f^4 \langle C_{\phi\phi} \rangle} \tag{9.3}$$

In the mass degenerate limit, this effective cross-section can be used to carefully compute the relic density with the input parameters, namely masses and couplings. This is done in the following chapter, but only in the non-degenerate limit, that amounts to neglect both $\langle C_{\phi\phi} \rangle$ and $\langle C_{\chi\phi} \rangle$.

Chapter III

Observational Evidence and Discussion

In the previous chapter we derived and studied the observables of the model by purely mathematical methods. However, up to here the constructed model is nothing more than an imaginary toy, which is completely detached from reality. In this chapter, we will bring the model to the real world and see how it can fit in the Universe. To do so, we will take a look at different cosmological observations and see how exactly we need to further shape the model and adjust it so that it is allowed to exist without contradicting any already present evidence. This will greatly restrict the parameter space of the model, which can either completely rule out the model or confine the parameters to given ranges, in which they can be more carefully searched.

10 Obtaining a Correct Dark Matter Abundance

As discussed before, it is a good approximation to say that the Dark Matter particle is non-relativistic both at decoupling and in the present day, even though the small energy dissipation from the self-interactions introduced here translate to Dark Matter being 'hotter' at decoupling than in the present day. This allows us to write

$$10^6 \, \frac{\hbar^2 c^3}{e^2} \, g^4 \, \frac{m^2}{64\,\pi (m^2 + M^2)^2} \approx \langle \sigma_A \, v_r \rangle \approx 3 \times 10^{-26} \frac{\mathrm{cm}^3}{\mathrm{s}} \,, \tag{10.1}$$

where we performed dimensional analysis to bring the expression to the correct units. We proceed to solve the equation for M. There are 4 different solutions, but only one satisfies the requirements for the mediator masses $M, m \in \mathbb{R}_{++}$. This is namely

$$M(g, m) = \sqrt{g^2 \, \zeta \, m - m^2} \,, \quad \zeta \approx 1.338 \times 10^{12} \mathrm{eV}. \tag{10.2}$$

Applying this condition makes a significant cut in the parameter space of the model. This is depicted in Fig. 10.1. An important consequence of $M > m$ and Eq. (10.2) is that a rough upper boundary for the Dark Matter mass is introduced, which is dependent on the coupling strength of the model

$$0 < m \lesssim g^2 \times 7 \times 10^{11} \mathrm{eV} \,. \tag{10.3}$$

With this in mind, we can now revisit the elastic scattering cross-section, substitute the necessary relation between the two masses, which we just found, and reduce the parameters in the expression to 3. Hence, $\sigma_{\mathrm{sc.}} = \sigma_{\mathrm{sc.}}(g, E_\nu, m)$, where E_ν is the energy of the incoming neutrino, formerly indicated with E_{p1}. We will not give the full expression as it does not provide any new

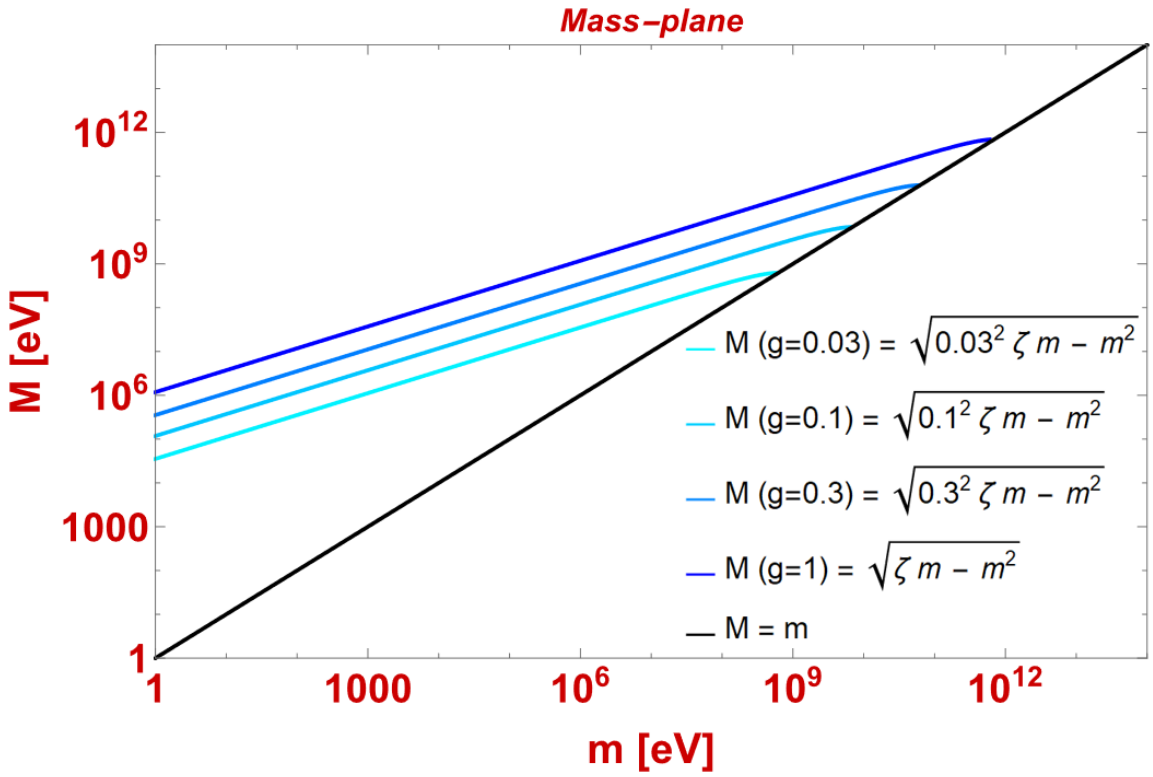

Figure 10.1: The mass-plane of the model with Dark Matter mass on x and mediator mass on y. The model has to stay above the black line and strictly on the blue lines. They describe the condition on the masses, which gives the correct abundance of Dark Matter, for different values of the coupling strength.

insight and is too lengthy. Instead, we go directly to plotting it (Fig. 10.2). As expected, the elastic scattering cross-section decreases approximately linearly with Dark Matter mass, which is to be expected for a relevant (third order in fields) interaction term. There are a few further features of the model, which are worthy of discussion, but we will wait to see in what other way we can constrain the model before discussing them.

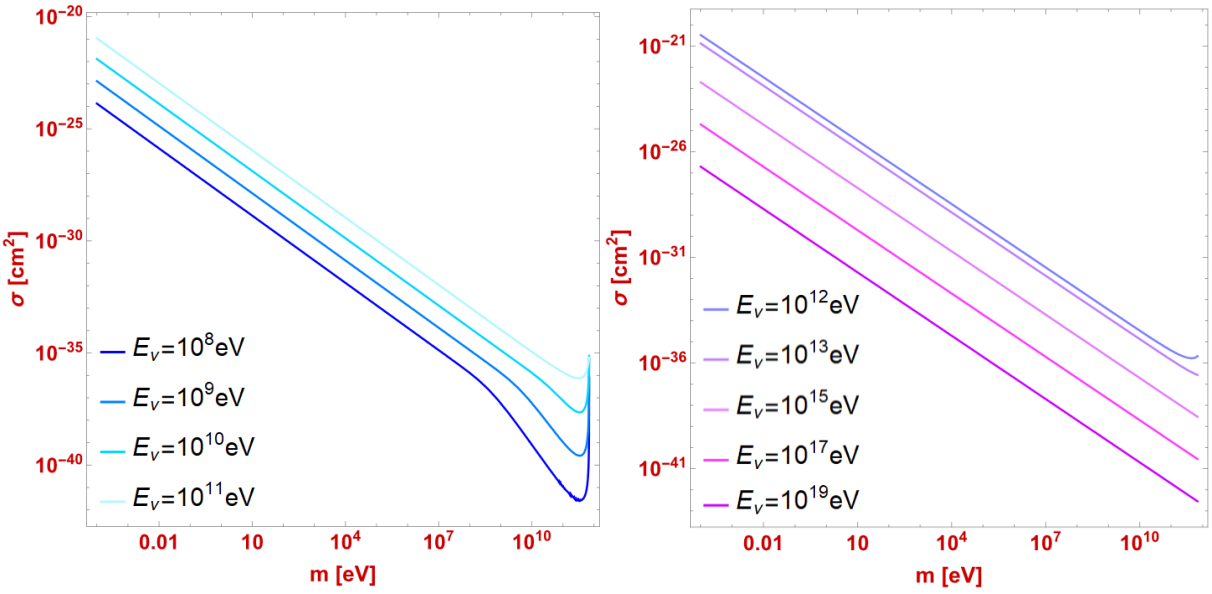

(a) (b)

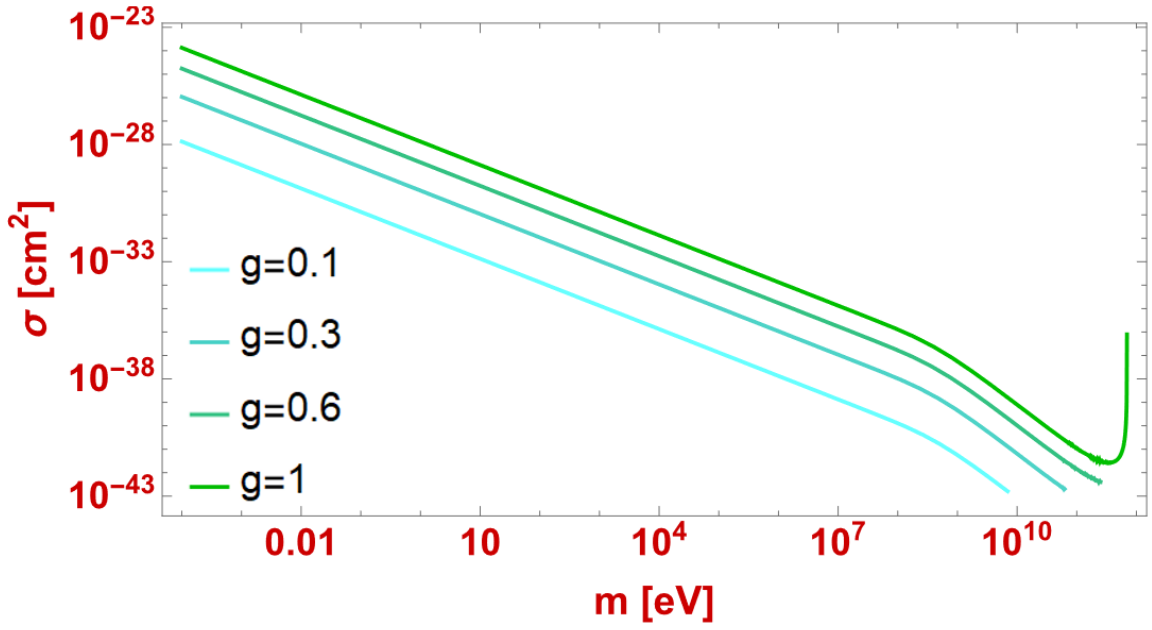

(c)

Figure 10.2: **(a)**, **(b)** The elastic scattering cross-section is plotted against the mass of the Dark Matter particle for a fixed coupling strength ($g = 1$). As we can see, the different lines represent different incoming neutrino energies and while plot (a) focuses on the lower-end, plot (b) focuses on the higher energies. **(c)** Again, the elastic scattering cross-section is depicted, but this time the neutrino energy is held constant at $E_\nu = 10^8$eV and the coupling strength is varied.

11 Further Observational Constraints

The two relevant interactions of Dark Matter with neutrinos of the model, described by Eq. (6.9), have been analysed mathematically and 'paired' together. It is now time to look a bit more in detail into the behaviour of the cross-sections and their dependence on the input parameters. Furthermore, observational data has to be examined and implemented in order to confine the model to the real world. The goal of this section is to:

(1) Constrain the model and its parameters to specific ranges. This is useful for testing the theory since it is much easier to examine a specific range as opposed to a full spectrum. Additionally, this provides a more specific energy scale on which the model is valid.

(2) Find detection signatures. This term points to very specific features of the model, which could potentially lead to very sharp and noticeable behaviour in the case that outgoing neutrinos from the aforementioned interactions are detected. This would be a sign that the model is on the right track. Conversely, it is possible to find detection signatures, which would specifically signal that the model is fundamentally wrong and not a good description of reality.

11.1 From Large Scale Structures

In the present day, interactions of neutrinos with other Standard Model (visible) particles and matter are somewhat well understood. These interactions have certain impacts on how the Universe is shaped (e.g. the scales on which neutrinos or other matter clusters). If we now consider a reality in which Dark Matter interacts with neutrinos, we can expect fundamental changes in the CMB and the structure formation of the Universe.[87–89] One one hand, introducing a non-collisionless Dark Matter (because it can interact weakly with itself) will result in suppression of the oscillation of the matter power spectrum of the CMB.[90] Data from the 2015 Planck satellite (Fig. 2.3a) survey was analysed and resulted in a relatively weak upper bound on the strength of the elastic scattering interaction.[91] Namely, the elastic scattering cross-section cannot be greater than $\sigma_{\text{sc.}} < 6 \times 10^{-40} \, (\frac{m}{\text{eV}}) \, \text{cm}^2$. On the other hand, neutrinos have a certain average frequency of interaction with visible matter, which translates to a certain mean free path. Allowing neutrinos to also interact with Dark Matter, which is highly abundant, will result in changes of the mean free path, which in turn will reduce the scale on which neutrinos tend to cluster around matter in the Universe. A stronger bound than the one mentioned earlier comes from analysis of the same Planck data, but this time paired with observations of Large Scale Structures from the Lyman-α forest (a series of absorption lines in the spectrum of a galaxy or any large observable structure).[92] This analysis[93] gives an upper boundary for the elastic scattering cross-section of $\sigma_{\text{sc.}} < 10^{-42} \, (\frac{m}{\text{eV}}) \, \text{cm}^2$ and this is the strongest boundary on the interaction strength as of today. It is possible that in the future even stricter constraints can be made based on observational data. It is important to note that in our model we assume that the elastic scattering cross-section is independent of temperature. This boundary is plotted in orange in Fig. 11.1.

11.2 From Neutrino Re-heating

We consider Weakly Interacting Massive Particles, which are thought to decouple from the early Universe at a time before the Big Bang Nucelosynthesis (BBN).[6] The BBN is thought to occur the latest at a temperature of $T \gtrsim 4\text{MeV}$.[94] At the same time, neutrinos decouple from electrons at a $T_1 \sim 2.3\text{MeV}$.[95] Lastly, as discussed in Chapter I, the CMB is emitted at a much later time

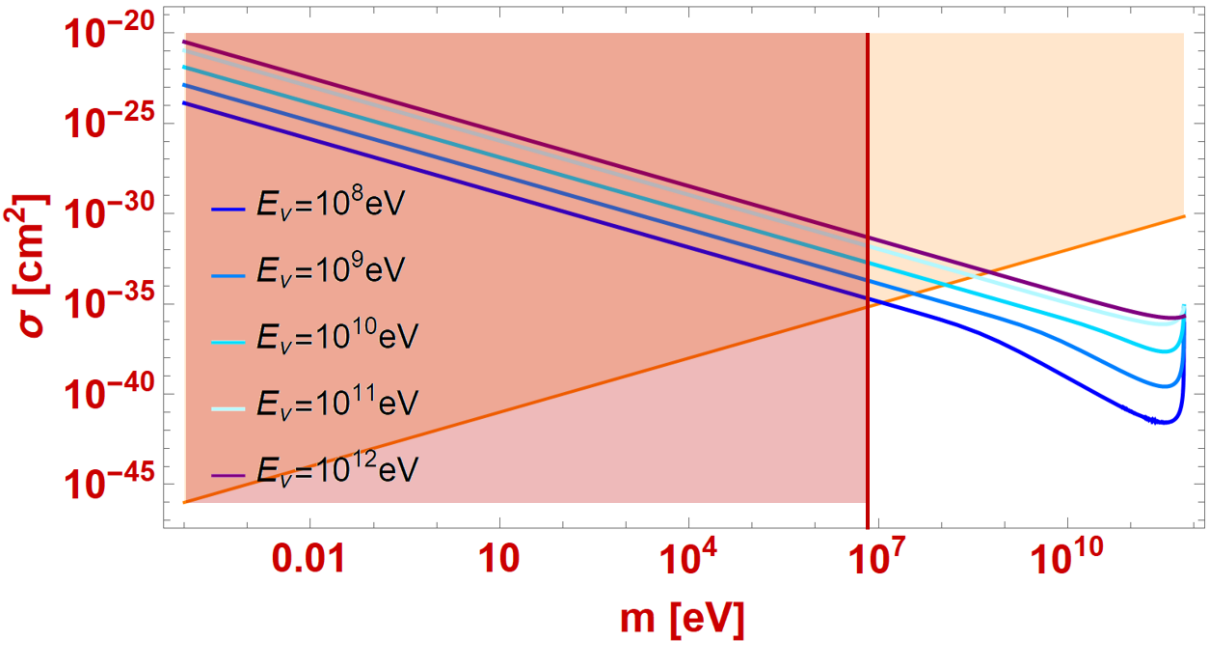

Figure 11.1: The elastic scattering cross-section is plotted against mass of the Dark Matter particle, identically to Fig. 10.2a. In addition, the orange line and shaded region represent the boundary due to LSS formation constraints and the forbidden region respectively. The red line and shaded region do the same for the boundaries derived from neutrino reheating bounds.

at temperature $T_2 \sim 1\text{eV}$.[31] At temperatures $T_2 < T < T_1$ it is possible to have Dark Matter annihilating into neutrinos. This could change the neutrino energy density in the early Universe, which would have significant impacts on the emission of the CMB and its power spectrum.[75] Since the mass of the Dark Matter determines the time at which it decouples, analysis of the Planck data of the CMB power spectrum can impose a lower boundary on the mass of the Dark Matter particle of a few MeVs.[96,97] This constraint complements well the one from LSS formation.

All of the boundaries discussed so far are depicted in Fig. 11.1. This restricts the model to only live in the small trapezoidal region on the bottom right of the figure. We now have a much better-defined range for the Dark Matter mass

$$\mathcal{O}(1\,\text{MeV}) \lesssim m \lesssim g^2 \times 7 \times 10^{11}\text{eV}\,. \tag{11.1}$$

In order to see how these constraints impact the model specifically and what they require for the parameters, we have to do a little more analysis.

12 Restrictions on the Parameter Space

In order to consider this model as plausible we have to show that it satisfies fully the constraints, which were imposed in the previous section. This means that for all configurations of sensibly selected parameters, the model must remain within the boundaries. The most obvious constraints that can be presented are the mass constraints, which have been partially discussed already. As can be seen from Eq. (10.2), the boundaries of both masses are dependent on the coupling strength g. We will now try to translate the mass boundaries to rough g-boundaries and ideally

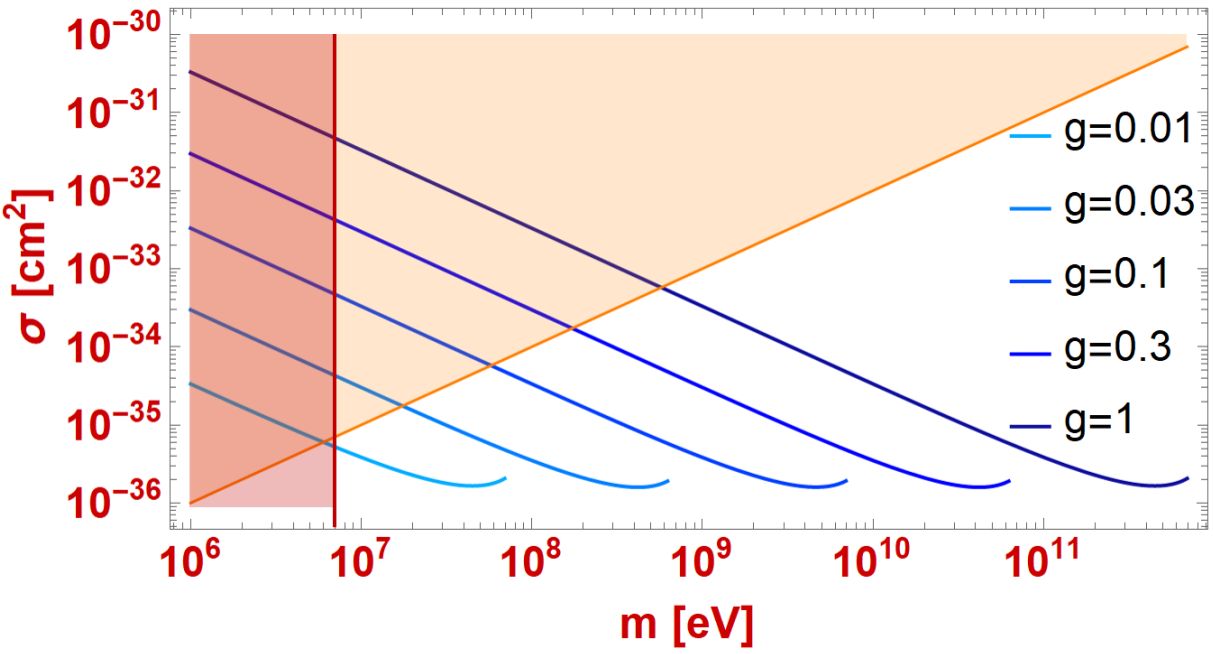

Figure 11.2: Elastic scattering cross-section is plotted against Dark Matter mass for different coupling parameters g. The neutrino energies are taken to give maximal cross-sections at the specified coupling parameters, thus being most likely to contradict observations (See Fig. 12.1). The figure is zoomed on the allowed region and the observational constraints are shown in the same way as in Fig. 11.1. As can be seen, the cross-section for $g = 1$ currently is in contradiction with observations for $m \lesssim 1$GeV *Note:* The abrupt ends of the graphs depict the upper boundary of the Dark Matter mass, which varies with the coupling strength as in (11.1).

arrive at a well-defined region in the parameter space where the model can exist. It should be pointed out that the fundamental parameters of the model are the Dark Matter and mediator mass m and M respectively, and the coupling strength parameter g. The possibility for an elastic scattering or an annihilation interaction could also be governed by energies, momenta, and other interaction parameters and so the exact elastic scattering cross-section may vary from one interaction to another. Therefore, we must find a region in the m-M-g parameter space where the elastic scattering cross-section satisfies the discussed observational constraints for all physically achievable interaction parameters. Luckily, after approximations, the only interaction parameter for which we have to worry is the neutrino energy E_ν.

This means that for all neutrino energies found in the cosmos, the elastic scattering cross-section must not exceed a given value, which is imposed by Large Scale Structure Formation, as explained in the previous section. As can be deduced from Figures 10.2a and 10.2b, there exists a maximum for the cross-section with respect to the neutrino energy. For $g = 1$, this maximum occurs at an energy of about $E_\nu \sim 1$ TeV, which is also roughly the upper boundary for the Dark Matter mass. This can be considered to be a fairly 'usual' and accessible energy for a neutrino, especially in the present-day Universe. Analysis of the cross-section as in Eq. (7.13) in the region of interest does not reveal any additional critical points and so we can assume that as the global maximum (See Fig. 12.1). It turns out that for different coupling parameter values, the maximum cross-section occurs at different neutrino energies, which are depicted in Figure 12.1.

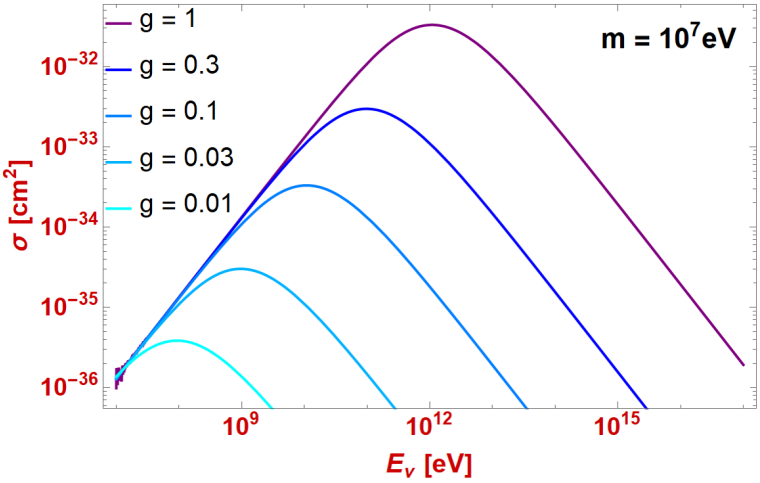

Figure 12.1: Elastic scattering cross-section plotted against incoming neutrino energy. The Dark Matter mass is fixed and the coupling strength parameter g is varied to demonstrate varying maxima.

This result is extremely important because it can be used to constrain the model further. At given values of g, there are specific energies for which the scattering cross-section is maximal for all relevant Dark Matter masses. Therefore, also the model is most likely to be in contradiction with the constraint from Large Scale Structures, which produces an upper boundary for the cross-section. In other words, if we ensure the model is not in contradiction with observations at that given neutrino energy, then it will not be in contradiction at any other neutrino energy. This can be seen in Figure 11.1 – so that they are not in contradiction with observations, the blue lines must not overlap with neither the orange region (upper boundary on the elastic cross-section from LSS), nor the red region (lower bound on Dark Matter mass from Neutrino Reheating). Now, the purple line (denoting $E_\nu \sim 10^{12}$eV) appears to give a largest cross-section for $g = 1$ and due to the linear-in-mass constraint from LSS, it also corresponds to the smallest range of admissible Dark Matter masses. The goal currently is to exclude as many regions from the parameter space as possible. Hence, from now on, for every set of parameters g, m, M, we will pick out and use only the energy, which results in a maximal elastic scattering cross-section. We can utilise this to proceed and see how we can constrain the remaining parameters further.

It is now more useful to look at Figure 11.2 in order to understand how we must move forward if we want to obtain a plausible model. There are two parameters left to be varied and they are namely the Dark Matter mass m and the coupling parameter g since the mediator mass M was shown to depend on them as in Eq. (10.2). We must ensure that for all combinations of these parameters the elastic scattering cross-section does not contradict observations.

As can be seen from Figure 11.2, if we select $g \lesssim 0.012$, the model is very much safe as the region, where the elastic scattering cross-section would be in contradiction, cannot be accessed because there is a lower boundary on the Dark Matter mass from Neutrino Reheating. This choice of g, however, lowers the upper boundary of the Dark Matter mass as in the inequality (11.1). On the other hand, if we select $g \gtrsim 0.012$, we must introduce a new lower boundary for the Dark Matter mass m, which is stronger than the boundary from Neutrino Reheating [a]. The exact value of the coupling parameter where this new boundary has to be introduced could be studied in more detail and found more precisely if the lower boundary of the Dark Matter mass from Neutrino Reheating is determined more precisely. These results can be extended and summarised by denoting a specific region in the $g - m$ plane, where the model can exist and not be in contradiction with neither of the observations described in the previous section. This is done in Figure 12.2. It is important to note that a lower boundary on g has to be imposed (so that the inequality (11.1) is proper) and this lower boundary would be more or less consistent

[a] The actual function for that boundary cannot be found analytically and is instead approximated numerically.

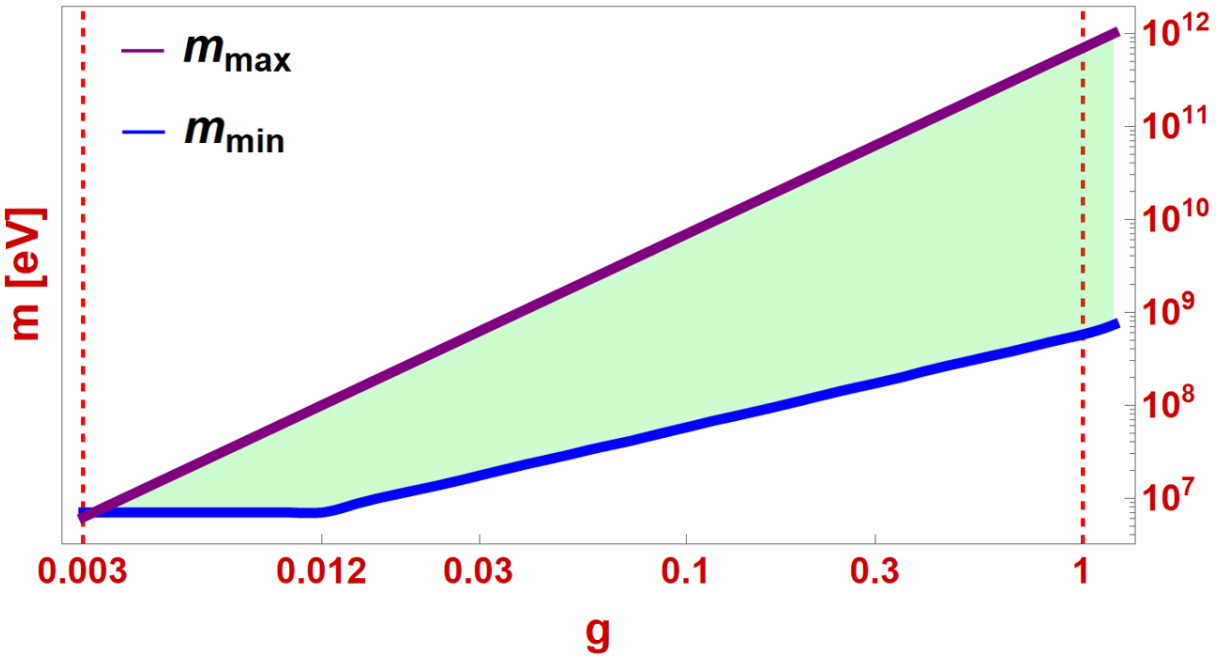

Figure 12.2: Coupling parameter-Dark Matter mass m plane. The blue and purple lines represent lower and upper boundaries of the Dark Matter mass respectively. The model can exist only in the light-green shaded region if it is to not contradict any observational constraints. The boundaries for $g \lesssim 0.012$ are identical to those in (11.1). However, a new boundary is introduced for $g \gtrsim 0.012$ so that the model is not in contradiction with the constraint from Large Scale Structures. The dashed red lines depict an expected region for a coupling parameter of a Weak interaction, which also satisfies a perturbative theory.

with the lower boundary that one would expect for a coupling parameter of an interaction on the Weak scale. On the other hand, the model does not imply a specific upper boundary on g, but one would not expect $g > 1$ for an interaction around and below the Weak scale. Additionally, any perturbative theory in g (e.g. the Dyson series based on which the scattering matrix is computed) is on the safe side in terms of validity if $g < 1$. Perhaps a better dimensionless constant for a perturbative theory is the $\frac{g^2}{4\pi}$, which would allow coupling parameters up to $g \sim 2$.[60] Furthermore, the condition $g < 1$ guarantees that the given in Figures 7.1 and 8.1 two-vertex diagrams result in leading terms in the amplitude. In this way, any higher order loop diagrams are essentially suppressed. Finally, a connected set of allowed parameter values for g and m can be constructed (light-green region in Figure 12.2) and the mediator mass M parameter can be found for any point of that set by Eq. (10.2), which can now be considered an injective mapping $\mathbb{R}^2 \to \mathbb{R}$.

An alternative approach

What was done so far is to utilise the correct abundance condition as in Eq. (10.2), substitute it back in the expression for the cross-section (7.13), and arrive at conclusions. This approach has its perks in terms of simplicity, but it would be also useful to visualise a region, in which the model is allowed to exist, in a way that puts the Dark Matter and mediator masses on equal footing. To do that, we can solve Eq. (10.1) for the coupling parameter g and proceed to substitute in in the expression for the elastic scattering cross-section. Once that is done,

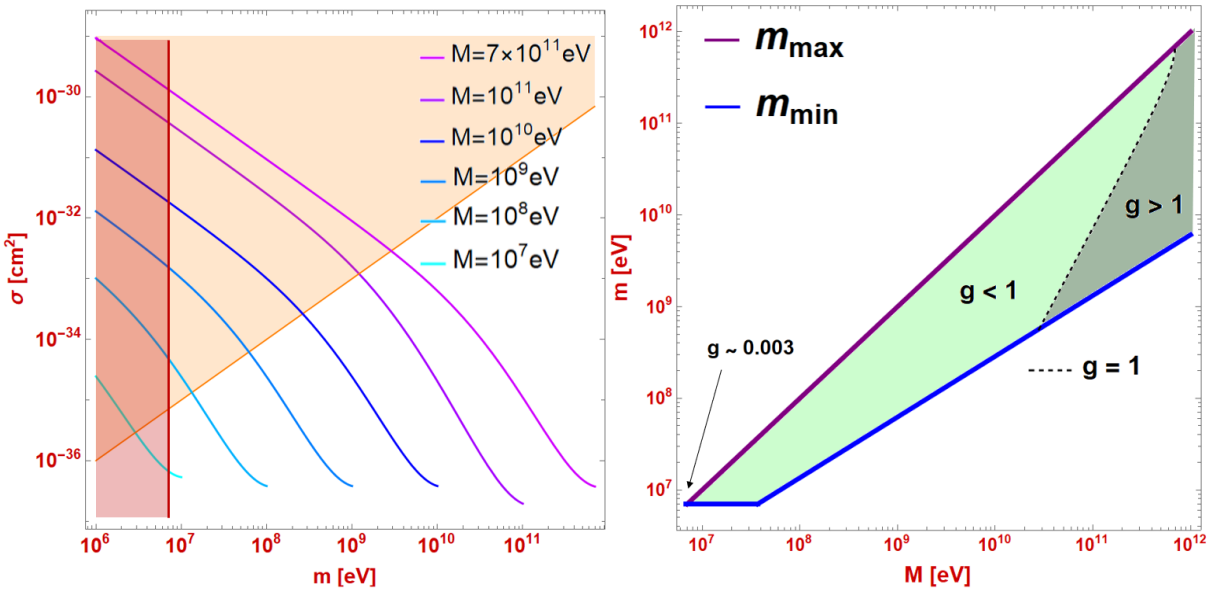

(a) (b)

Figure 12.3: **(a)** Similarly to Fig. 11.2, the elastic scattering cross-section is plotted against the Dark Matter mass for varying mediator mass M. The neutrino energies for each line are picked to give a maximal cross-section. The orange and red regions depict the same boundaries. **(b)** Similarly to Fig. 12.2, the region in which the model can exist without contradicting observations is shown in light-green between the lower (blue) and upper (purple) boundaries for the Dark Matter mass. The grey dashed line depicts $g = 1$ and the grey region to the right of it ($g > 1$) can be excluded/neglected by interaction strength arguments.

we can examine the dependence of the scattering cross-section on the mediator mass in more detail (See Fig. 12.3a). When it comes to selecting energies of the incoming neutrino, we can now use a similar logic to what we did for g. Namely, different neutrino energies give maximal cross-sections for different configurations of model parameters M, m, g. This is studied and all presented results involve only energies which give maximal cross-sections. As we did before, we can state how the lower boundary for the Dark Matter mass from Neutrino reheating needs a stronger replacement after a certain point ($M \sim 30$MeV) as the boundary from Large Scale Structures becomes stronger. This allows for the construction of Figure 12.3b, which showcases the allowed region in the mass-plane. The lower boundary (blue line on Fig. 12.3b) is safely in the non-degenerate-in-mass limit, except for the low-mass region where the two boundaries meet and possible altering of the allowed region could be necessary of co-annihilations are taken into account. Once again, every point of the connected set corresponds to a (non-unique) coupling parameter g. The intersection point in the bottom-left corner of Figure 12.3b corresponds to the same corner from Figure 12.2 where $g \sim 0.003$. In addition, we can make use of the expectation that the coupling parameter does not exceed $g \sim 1$ to further restrict the parameter space, as depicted by the grey line and region.

13 Detection Signatures

Now that we are fully acquainted with the model, its properties, and parameters, it is time to figure out how exactly we can find out if the model is a correct description of reality, partially

correct or fully incorrect. The features of the model, that would influence any relics from the early Universe like the CMB, have already been fully covered and we will focus solely on detection of interactions that have taken place in the present day. We can further divide the detection into detection of scattering and detection of annihilation.

As stated previously, the model of the thesis allows weak interactions of Dark Matter with itself. This leads to annihilation into neutrinos. The law of conservation of energy dictates that the outgoing neutrinos (in opposite directions) must possess an energy, which is very similar to the mass of the Dark Matter particle m. As discussed in the Chapter I, Dark Matter clusters in certain structures throughout the Universe. Therefore, a careful examination of the neutrino fluxes, which are coming from the direction of the selected object would reveal a slight bump at approximately the mass of the Dark Matter. The energies, which must be surveyed are defined by the mass boundaries as discussed in the previous section. Some facilities, which can prove useful in that case, are depicted in Fig. 3.1.

Additionally, scattering of Dark Matter with neutrinos could occur in relatively large scales near certain astronomical objects, which have also been discussed in Chapter I. These interactions would be harder to detect and would require very good precision in the detection, which is almost impossible with the available nowadays detectors. Nevertheless, one can calculate the expected flux from a specific location due to that interaction and try to find knee-like features, which would be due to the cross-sectional maxima at a given neutrino energy, as depicted in Figure 12.1. These features might be easier to find especially if the data is compared with data from a direction in which the interaction is expected to take place less often. Again, all of this would require very precise examination of the neutrino fluxes reaching Earth, would be quite challenging with the current detection techniques known to particle physicists. The biggest hope lies within the IceCube facility and the newer generation of neutrino detectors.

14 Direct Searches

So far we have been only discussing indirect evidence for the existence of Dark Matter and have made rough conclusions on how the existence of Dark Matter can be indirectly showcased. Although indirect evidence can be very convincing and at the same time relatively easier to find, it is always also worthy to discuss the possible direct detection of WIMPs. A successful detection of a Dark Matter particle will truly start a new era of Physics because direct detection is linked to direct measurement of properties, which in turn can shine a lot of light on the nature of Dark Matter. Obviously, the main challenge for detection is that it requires a well-understood interaction with a particle within a detector. Moreover, the interaction has to occur with a relatively large probability. Fortunately, by WIMPs are thought to interact weakly, which allows them to interact with leptons and possible other fermions and combinations thereof. In particular, WIMP-nucleon interactions are of interest, to a large extent due to the significant understanding and abundance of nucleons. Additionally, WIMP-lepton interactions can also be linked to nucleon coupling from loop diagrams.[98] It should be stated that local Dark Matter densities and velocity distributions play a significant role in direct detection and the relative lack of understanding of these parameters at Earth-based detectors makes direct detection even more complicated and coupling to flavoured particles (quarks and leptons) imposes additional conditions on the interaction mediator.[77]

As of today, there is no single confirmed detection of a WIMP-nucleon interaction. However, failed detection experiments can still be used to constrain the strength of a possible interaction of that sort. Some of the detection techniques used currently for WIMP detection are ultra-

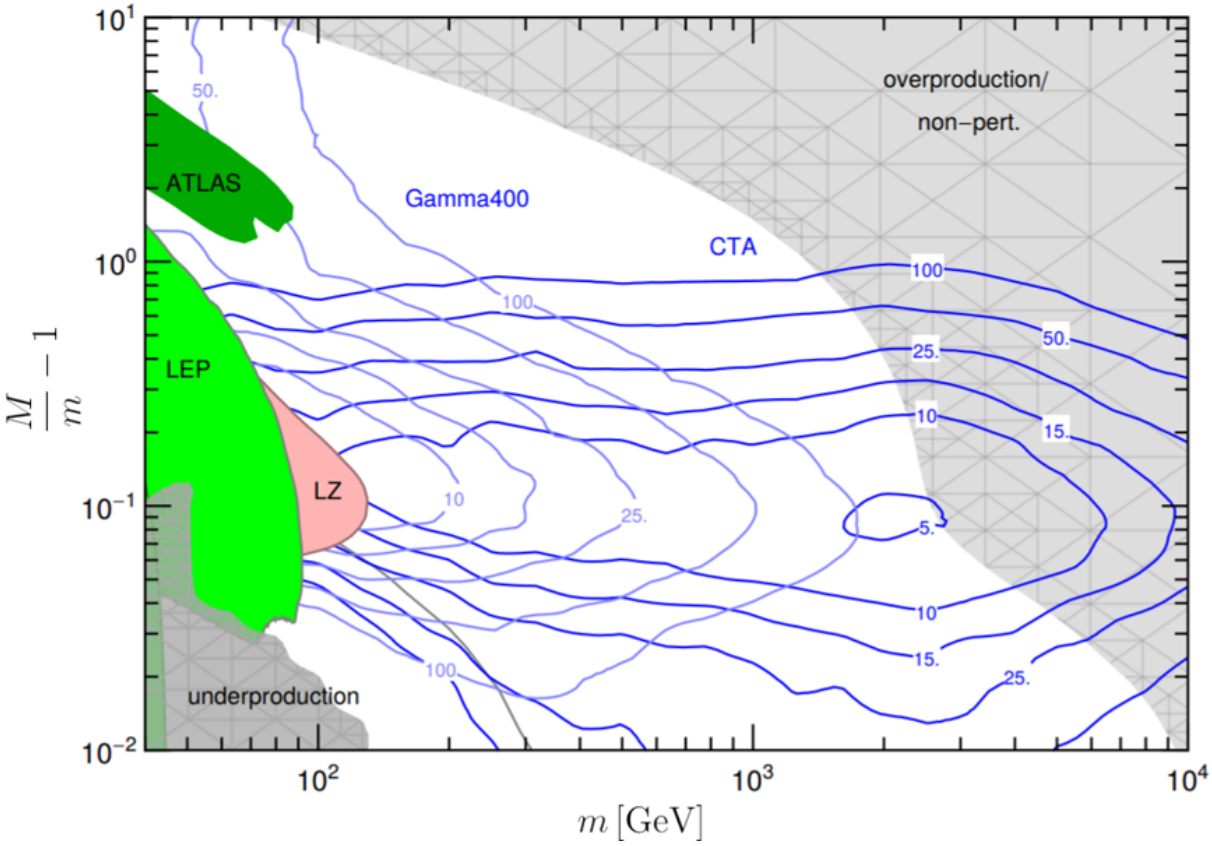

Figure 14.1: An equivalent of a mediator-Dark Matter mass plane for a *Majorana* fermion Dark Matter and complex scalar mediator, which is the closest possible variation to the model of this thesis.. The green regions are excluded from collider searches. The pink region could be tested in the future with the LUX-ZEPLIN facility. Taken from *Garny et al, 2015*.[77]

cold semiconductor detectors, noble gas scintillators, crystal scintillators, bubble chambers, etc. The current strongest limits are set by the SuperCDMS experiment[99] (cryogenic semiconductor detectors) and the LUX experiment[100] (xenon scintillator) and will not be discussed in detail here as they are only marginally relevant since this thesis focuses on WIMP-lepton interactions.

In the past two decades, there have been four independent collaborations, which have signalled a Dark Matter detection event. Half of them have been shown to be false alarms, but there are two detections, which are still under investigation and the sides involved cannot agree on a single conclusion.[101] These are detections performed by DAMA and CDMS-Si, which both claim to detect a signal, which could be produced by a WIMP-nucleon interaction with a reasonable certainty.[101, 102] Both signal a detection of a WIMP in the GeV range, which is very well accommodated in our model as well. Both have also been ruled out by the aforementioned SuperCDMS and LUX experiment constraints, but there is still some lingering plausibility that WIMPs really were detected.[103] Currently, hope lies within the next generation of WIMP-nucleon detectors like LUX-ZEPLIN (could probe a fermionic Dark Matter and complex scalar mediator model like in Fig. 14.1) and DARWIN, which are expected to be operational in the next decade.[104, 105]

WIMP-lepton interactions can also be used for direct detection of Dark Matter. As previously stated, since left-handed leptons come in $SU(2)$ doublets, the interaction Lagrangian (6.9) allows

charged lepton interactions as well. These are normally not observed in the cosmos or at least in large scales. This does not rule out the possibility for WIMP-lepton interactions, but simply provides a constraint on the interaction strength like we have seen a lot so far. Some of these can be seen in Figure 14.1.

If Dark Matter interacts with Standard Model particles, like we have allowed it to in the model of this thesis, a good question to ask is why has not Dark Matter ever been detected in collider experiments? The Large Hadron Collider (LHC) can reach energies of $\mathcal{O}(1\text{TeV})$ and our model can be considered to live entirely below this energy scale. Additionally, the Large Electron-Positron Collider (LEP) can achieve energies of about a couple hundred GeVs. The lack of observation in the largest collider facilities can also be used for restriction of parameter spaces. A mediator can be produced only in the mass-degenerate limit and it can subsequently undergo a fast decay to Dark Matter. It should be added that the lack of direct observation does not mean a Dark Matter or a mediator particle was not produced – it means the leptons (most likely neutrinos) were simply not detected and flavour can play a significant role in that detection.[77] Examples of limits imposed by such collider searches are depicted in Figure 14.1.

Chapter IV

Conclusions

Revealing the secrets of Dark Matter has been a main scientific goal for almost half a century now. The knowledge they hide is essential for the understanding of the Universe and its history. Should it be a thermal relic of the early Universe, Dark Matter is also thought to hold information about the Universe from before the emission of the CMB and even the BBN – an epoch, about which we know very little currently.[6]

In this thesis, we began by introducing Dark Matter, evidence for its existence, famous possible particle and non-particle candidates, and how it could have become the crucial part of the Universe that it is today. We also reviewed neutrinos, their detection, and what secrets it could reveal about Dark Matter. Some of the basic mathematical tools from Quantum Field Theory were reviewed for better understanding of how exactly the amplitudes and cross-sections are derived and computed. We considered and examined a simplified model, which effectively tests the interactions between these two particles. Feynman diagrams and amplitudes were constructed and computed. Cross-sections were extracted based on these and also studied in detail. By imposing a multitude of constraints on the model, which come from cosmological observations, we showed how they translate to the parameters of the model and what they mean. Additionally, we showed what astronomical observations could be linked to the plausibility of the model and in what energy ranges such searches should be undertaken. On the grand scheme of the history of the Universe, we probe and take information from roughly three epochs – the decoupling of Dark Matter, the interactions of Dark Matter before the emission of the CMB, and the present-day Universe and the interactions of Dark Matter in it. The first one gives information about the self-interaction strength of Dark Matter as based on the energy density of Dark Matter in the Universe. Upon careful examination of early Universe relics, the second one provides details about the gravitational interactions of Dark Matter with visible matter but also about possible weak interactions like the ones we discussed in this thesis. The interactions of Dark Matter in that epoch leave a permanent footprint on the CMB, which can then be surveyed for indirect evidence, but also give constraints on these possible interactions. The measurement of the energy density of Dark Matter is arguably the most important piece of information on Dark Matter that is available and is also determined by detailed studies of the CMB. The last epoch tells a little bit about how Dark Matter interacts with itself and other particles and most importantly, we must study this epoch extensively if direct evidence is ever to be found for the existence of Dark Matter. All three information sources are combined and based on them and their analysis, we made predictions about the nature of Dark Matter under significant assumptions.

The Dirac Dark Matter and complex scalar mediator model falls under the rather large

umbrella of the Lambda Cold Dark Matter model (ΛCDM). Alternatives like a modified theory of gravity exist, which was briefly explained in Chapter I, but ΛCDM is currently considered to be the only 'standard model of the Big Bang', which can explain the observed structure and dynamics of the Universe. The coldness of Dark Matter was reviewed before and this specific property was utilised on several occasions for computational simplification. The lambda stands for dark energy, which is very marginally related to our model in the sense that its presence is required for the correct understanding of energy densities in the Universe. ΛCDM holds high hopes for the future with the main missing components being the full detection and understanding of these *dark* elements of the Universe, which comprise only some $\sim 95\%$ of it.

At first it may seem like this approach resembles searching for a needle in a haystack and this is not far from the truth. The model is very specific and assumes very specific properties of the Dark Matter particle and the way it interacts. There are plenty of other possibilities and there is no evidence so far that would specifically mean one model is preferred over the other. Therefore, it is important that all possibilities are considered, analysed, and taken into account. Even if this model can be compared to searching for a needle in a haystack, it is a search nonetheless. In addition, careful analysis can be exploited to extract information about the plausibility of this model and similar ones, thus giving an indication whether the needle is in this corner of the haystack or not close at all.

There are several aspects of the model and issues that may arise, which were mentioned throughout the thesis, but not discussed in detail. Firstly, interactions of Dark Matter with charged leptons bring a whole bag of additional complications. A consideration of the full Standard Model and the provided extension for Dark Matter can result in Dark Matter coupling to nucleons or the electromagnetic sector. Additional limits must be imposed from observation and direct searches to restrict these interactions and subsequently the parameter space of the model. These are very important to be taken into account for a more detailed study of the direct detection of this model. Secondly, flavours of neutrinos and leptons were not covered in the thesis but are also worthy of further examination in a more detailed study of Dark Matter detection. Just like charged lepton interactions, adding flavours to the model does not change the underlying general properties of the model, but it introduces a colour/flavour to the mediator. The fact that Dark Matter and the mediator are massive can additionally require an extension, which would cover mixing with the Higgs boson and a mass generation mechanism. Lastly, a major subtopic, which should be studied for a complete comprehension of the model is the mass-degenerate regime. When the two particle masses are very similar, the production of Dark Matter in the early Universe is altered and the so-called co-annihilation channels must be studied as well. These will not necessarily give a spectacular new result in terms of model behaviour but will require an adaptation and adjustment in the $M \sim m$ region of the parameter space.

In any case, high hopes for the solution to the Dark Matter problem lie within new generations of observational tools in both gravitational wave and neutrino astronomy. With more precise measurements, models like this one can be examined in a lot more detail and hopefully the model that describes Dark Matter correctly is revealed, even if it is not this one specifically.

Bibliography

[1] H. Poincaré, "The milky way and the theory of gases," *Popular Astronomy*, vol. 14, pp. 475–488, 1906.

[2] J. C. Kapteyn, "First attempt at a theory of the arrangement and motion of the sidereal system," *The Astrophysical Journal*, vol. 55, p. 302, 1922.

[3] J. H. Oort *et al.*, "The force exerted by the stellar system in the direction perpendicular to the galactic plane and some related problems," *Bulletin of the Astronomical Institutes of the Netherlands*, vol. 6, p. 249, 1932.

[4] F. Zwicky, "Die rotverschiebung von extragalaktischen nebeln," *Helvetica physica acta*, vol. 6, pp. 110–127, 1933.

[5] V. Trimble, "Existence and nature of dark matter in the universe," *Annual review of astronomy and astrophysics*, vol. 25, no. 1, pp. 425–472, 1987.

[6] G. B. Gelmini, "Tasi 2014 lectures: the hunt for dark matter," *arXiv preprint arXiv:1502.01320*, 2015.

[7] L. M. Brown and L. Hoddeson, *The birth of particle physics*. CUP Archive, 1986.

[8] V. C. Rubin and W. K. Ford Jr, "Rotation of the andromeda nebula from a spectroscopic survey of emission regions," *The Astrophysical Journal*, vol. 159, p. 379, 1970.

[9] K. C. Freeman, "On the disks of spiral and s0 galaxies," *The Astrophysical Journal*, vol. 160, p. 811, 1970.

[10] V. C. Rubin, W. K. Ford Jr, and N. Thonnard, "Rotational properties of 21 sc galaxies with a large range of luminosities and radii, from ngc 4605/r= 4kpc/to ugc 2885/r= 122 kpc," *The Astrophysical Journal*, vol. 238, pp. 471–487, 1980.

[11] A. Borriello and P. Salucci, "The dark matter distribution in disc galaxies," *Monthly Notices of the Royal Astronomical Society*, vol. 323, no. 2, pp. 285–292, 2001.

[12] K. Begeman, A. Broeils, and R. Sanders, "Extended rotation curves of spiral galaxies: Dark haloes and modified dynamics," *Monthly Notices of the Royal Astronomical Society*, vol. 249, no. 3, pp. 523–537, 1991.

[13] R. Carlberg and W. L. Freedman, "Dissipative models of spiral galaxies," *The Astrophysical Journal*, vol. 298, pp. 486–492, 1985.

[14] J. F. Navarro and M. Steinmetz, "Dark halo and disk galaxy scaling laws in hierarchical universes," *The Astrophysical Journal*, vol. 538, no. 2, p. 477, 2000.

[15] B. Robertson, N. Yoshida, V. Springel, and L. Hernquist, "Disk galaxy formation in a λ cold dark matter universe," *The Astrophysical Journal*, vol. 606, no. 1, p. 32, 2004.

[16] P. Salucci and A. Burkert, "Dark matter scaling relations," *The Astrophysical Journal Letters*, vol. 537, no. 1, p. L9, 2000.

[17] E. van Uitert, H. Hoekstra, T. Schrabback, D. G. Gilbank, M. D. Gladders, and H. Yee, "Constraints on the shapes of galaxy dark matter haloes from weak gravitational lensing," *Astronomy & Astrophysics*, vol. 545, p. A71, 2012.

[18] L. A. Moustakas and R. B. Metcalf, "Detecting dark matter substructure spectroscopically in strong gravitational lenses," *Monthly Notices of the Royal Astronomical Society*, vol. 339, no. 3, pp. 607–615, 2003.

[19] M. Girardi, A. Biviano, G. Giuricin, F. Mardirossian, and M. Mezzetti, "Velocity dispersions in galaxy clusters," *The Astrophysical Journal*, vol. 404, pp. 38–50, 1993.

[20] F. Zwicky, "On the masses of nebulae and of clusters of nebulae," *The Astrophysical Journal*, vol. 86, p. 217, 1937.

[21] F. Kahlhoefer, K. Schmidt-Hoberg, M. T. Frandsen, and S. Sarkar, "Colliding clusters and dark matter self-interactions," *Monthly Notices of the Royal Astronomical Society*, vol. 437, no. 3, pp. 2865–2881, 2014.

[22] D. Clowe, M. Bradač, A. H. Gonzalez, M. Markevitch, S. W. Randall, C. Jones, and D. Zaritsky, "A direct empirical proof of the existence of dark matter," *The Astrophysical Journal Letters*, vol. 648, no. 2, p. L109, 2006.

[23] S. W. Allen, A. E. Evrard, and A. B. Mantz, "Cosmological parameters from observations of galaxy clusters," *Annual Review of Astronomy and Astrophysics*, vol. 49, pp. 409–470, 2011.

[24] O. Lahav and A. R. Liddle, "Review of particle physics," *Physics letters B*, vol. 592, no. 1-4, pp. 206–214, 2004.

[25] J. Han, Z. Wen, Z. Yuan, and T. Hong, "Identification of clusters of galaxies and physical properties of clusters and their member galaxies," *Chinese Science Bulletin*, vol. 64, no. 15, pp. 1583–1597, 2019.

[26] J. Estrada, E. Sefusatti, and J. A. Frieman, "The correlation function of optically selected galaxy clusters in the sloan digital sky survey," *The Astrophysical Journal*, vol. 692, no. 1, p. 265, 2009.

[27] W. J. Percival, S. Cole, D. J. Eisenstein, R. C. Nichol, J. A. Peacock, A. C. Pope, and A. S. Szalay, "Measuring the baryon acoustic oscillation scale using the sloan digital sky survey and 2df galaxy redshift survey," *Monthly Notices of the Royal Astronomical Society*, vol. 381, no. 3, pp. 1053–1066, 2007.

[28] D. J. Eisenstein, I. Zehavi, D. W. Hogg, R. Scoccimarro, M. R. Blanton, R. C. Nichol, R. Scranton, H.-J. Seo, M. Tegmark, Z. Zheng, *et al.*, "Detection of the baryon acoustic peak in the large-scale correlation function of sdss luminous red galaxies," *The Astrophysical Journal*, vol. 633, no. 2, p. 560, 2005.

[29] B. Ryden, *Introduction to cosmology*. Cambridge University Press, 2017.

[30] W. Hu, "Structure formation with generalized dark matter," *The Astrophysical Journal*, vol. 506, no. 2, p. 485, 1998.

[31] P. Noterdaeme, P. Petitjean, R. Srianand, C. Ledoux, and S. López, "The evolution of the cosmic microwave background temperature-measurements of tcmb at high redshift from carbon monoxide excitation," *Astronomy & Astrophysics*, vol. 526, p. L7, 2011.

[32] P. A. Ade, N. Aghanim, M. Arnaud, M. Ashdown, J. Aumont, C. Baccigalupi, A. Banday, R. Barreiro, J. Bartlett, N. Bartolo, *et al.*, "Planck 2015 results-xiii. cosmological parameters," *Astronomy & Astrophysics*, vol. 594, p. A13, 2016.

[33] R. Adam, P. A. Ade, N. Aghanim, Y. Akrami, M. Alves, F. Argüeso, M. Arnaud, F. Arroja, M. Ashdown, J. Aumont, *et al.*, "Planck 2015 results-i. overview of products and scientific results," *Astronomy & Astrophysics*, vol. 594, p. A1, 2016.

[34] M. Wilson and J. Silk, "On the anisotropy of the cosmological background matter and radiation distribution. i-the radiation anisotropy in a spatially flat universe," *The Astrophysical Journal*, vol. 243, pp. 14–25, 1981.

[35] E. L. Turner, "Gravitational lensing limits on the cosmological constant in a flat universe," *The Astrophysical Journal*, vol. 365, pp. L43–L46, 1990.

[36] N. Aghanim, Y. Akrami, M. Ashdown, J. Aumont, C. Baccigalupi, M. Ballardini, A. Banday, R. Barreiro, N. Bartolo, S. Basak, *et al.*, "Planck 2018 results. vi. cosmological parameters," *arXiv preprint arXiv:1807.06209*, 2018.

[37] M. Milgrom, "A modification of the newtonian dynamics as a possible alternative to the hidden mass hypothesis," *The Astrophysical Journal*, vol. 270, pp. 365–370, 1983.

[38] B. Famaey and S. S. McGaugh, "Modified newtonian dynamics (mond): observational phenomenology and relativistic extensions," *Living reviews in relativity*, vol. 15, no. 1, p. 10, 2012.

[39] S. S. McGaugh, "A tale of two paradigms: the mutual incommensurability of λcdm and mond," *Canadian Journal of Physics*, vol. 93, no. 2, pp. 250–259, 2015.

[40] T. Clifton, P. G. Ferreira, A. Padilla, and C. Skordis, "Modified gravity and cosmology," *Physics reports*, vol. 513, no. 1-3, pp. 1–189, 2012.

[41] J. R. Bond, G. Efstathiou, and J. Silk, "Massive neutrinos and the large-scale structure of the universe," *Phys. Rev. Lett.*, vol. 45, pp. 1980–1984, Dec 1980.

[42] J. Bond and A. Szalay, "The collisionless damping of density fluctuations in an expanding universe," 1983.

[43] S. D. White, C. S. Frenk, and M. Davis, "Clustering in a neutrino-dominated universe," *The Astrophysical Journal*, vol. 274, pp. L1–L5, 1983.

[44] G. Bertone, D. Hooper, and J. Silk, "Particle dark matter: Evidence, candidates and constraints," *Physics reports*, vol. 405, no. 5-6, pp. 279–390, 2005.

[45] S. Dodelson and L. M. Widrow, "Sterile neutrinos as dark matter," *Physical Review Letters*, vol. 72, no. 1, p. 17, 1994.

[46] S. Böser, C. Buck, C. Giunti, J. Lesgourgues, L. Ludhova, S. Mertens, A. Schukraft, and M. Wurm, "Status of light sterile neutrino searches," *Progress in Particle and Nuclear Physics*, vol. 111, p. 103736, 2020.

[47] R. D. Peccei and H. R. Quinn, "CP conservation in the presence of pseudoparticles," *Phys. Rev. Lett.*, vol. 38, pp. 1440–1443, Jun 1977.

[48] G. Fraser, A. Read, S. Sembay, J. Carter, and E. Schyns, "Potential solar axion signatures in x-ray observations with the xmm–newton observatory," *Monthly Notices of the Royal Astronomical Society*, vol. 445, no. 2, pp. 2146–2168, 2014.

[49] S. Martin, "A supersymmetry primer (hep-ph/9709356) preprint martin sp 1998," *Adv. Ser. Direct. High Energy Phys*, vol. 18, no. 1, 1997.

[50] T. Faber, Y. Liu, W. Porod, and J. Jones-Pérez, "Revisiting neutrino and sneutrino dark matter in natural susy scenarios," *Physical Review D*, vol. 101, no. 5, p. 055029, 2020.

[51] G. A. Gómez-Vargas, D. E. López-Fogliani, C. Muñoz, and A. D. Perez, "Mev-gev γ-ray telescopes probing axino lsp/gravitino nlsp as dark matter in the μ νssm," *Journal of Cosmology and Astroparticle Physics*, vol. 2020, no. 01, p. 058, 2020.

[52] B. J. Carr and S. W. Hawking, "Black Holes in the Early Universe," *Monthly Notices of the Royal Astronomical Society*, vol. 168, pp. 399–415, 08 1974.

[53] B. C. Lacki and J. F. Beacom, "Primordial black holes as dark matter: almost all or almost nothing," *The Astrophysical Journal Letters*, vol. 720, no. 1, p. L67, 2010.

[54] S. Clesse and J. García-Bellido, "Seven hints for primordial black hole dark matter," *Physics of the Dark Universe*, vol. 22, pp. 137–146, 2018.

[55] P. H. Frampton, M. Kawasaki, F. Takahashi, and T. T. Yanagida, "Primordial black holes as all dark matter," *Journal of Cosmology and Astroparticle Physics*, vol. 2010, no. 04, p. 023, 2010.

[56] G. Jungman, M. Kamionkowski, and K. Griest, "Supersymmetric dark matter," *Physics Reports*, vol. 267, no. 5-6, pp. 195–373, 1996.

[57] M. Cirelli, "Dark matter phenomenology," 2018.

[58] J. Niezing, "Freeze-in as a dark matter production mechanism," 2018.

[59] G. Gelmini and P. Gondolo, "Dm production mechanisms," *arXiv preprint arXiv:1009.3690*, 2010.

[60] S. Vogl, *Majorana Dark Matter: The Power of Direct, Indirect and Collider Searches*. PhD thesis, Technische Universitaet Muenchen, 2014.

[61] F. Reines and C. L. Cowan, "The neutrino," *Nature*, vol. 178, no. 4531, pp. 446–449, 1956.

[62] B. R. Martin and G. Shaw, *Nuclear and particle physics: an introduction*. John Wiley & Sons, 2019.

[63] C. Grupen, G. Cowan, S. Eidelman, and T. Stroh, *Astroparticle physics*, vol. 50. Springer, 2005.

[64] G. Sigl, "High energy astroparticle physics," *arXiv preprint astro-ph/0612240*, 2006.

[65] A. De Angelis and M. Pimenta, *Introduction to particle and astroparticle physics: multi-messenger astronomy and its particle physics foundations*. Springer, 2018.

[66] M. Tanabashi and et al. (Particle Data Group), "Light unflavoured mesons," *Phys. Rev. D*, vol. 98, no. 030001, 2018-2019.

[67] V. Berezinsky, "High energy neutrino astronomy," *Nuclear Physics B-Proceedings Supplements*, vol. 229, pp. 243–250, 2012.

[68] M. G. Aartsen, R. Abbasi, Y. Abdou, M. Ackermann, J. Adams, J. Aguilar, M. Ahlers, D. Altmann, J. Auffenberg, X. Bai, *et al.*, "First observation of pev-energy neutrinos with icecube," *Physical review letters*, vol. 111, no. 2, p. 021103, 2013.

[69] M. Vecchi and A. M. van den Berg, "Particle detection in astroparticle physics," *University of Groningen*, vol. 2, 2020.

[70] W. H. Press and D. N. Spergel, "Capture by the sun of a galactic population of weakly interacting, massive particles," *The Astrophysical Journal*, vol. 296, pp. 679–684, 1985.

[71] T. Evans, "Notes on wick's theorem," 2018.

[72] D. Tong, *Quantum Field Theory*. University of Cambridge, 2006.

[73] K. Kumericki, "Feynman diagrams for beginners," *arXiv preprint arXiv:1602.04182*, 2016.

[74] G. Bertone and T. M. Tait, "A new era in the search for dark matter," *Nature*, vol. 562, no. 7725, pp. 51–56, 2018.

[75] A. Olivares-Del Campo, C. Bœhm, S. Palomares-Ruiz, and S. Pascoli, "Dark matter-neutrino interactions through the lens of their cosmological implications," *Physical Review D*, vol. 97, no. 7, p. 075039, 2018.

[76] P. Hernandez, "Neutrino physics," *arXiv preprint arXiv:1708.01046*, 2017.

[77] M. Garny, A. Ibarra, and S. Vogl, "Signatures of majorana dark matter with t-channel mediators," *International Journal of Modern Physics D*, vol. 24, no. 07, p. 1530019, 2015.

[78] C. Boehm, A. Djouadi, and M. Drees, "Light scalar top quarks and supersymmetric dark matter," *Physical Review D*, vol. 62, no. 3, p. 035012, 2000.

[79] E. Bagnaschi, O. Buchmueller, R. Cavanaugh, M. Citron, A. De Roeck, M. Dolan, J. Ellis, H. Flächer, S. Heinemeyer, G. Isidori, *et al.*, "Supersymmetric dark matter after lhc run 1," *The European Physical Journal C*, vol. 75, no. 10, p. 500, 2015.

[80] J. Kopp, L. Michaels, and J. Smirnov, "Loopy constraints on leptophilic dark matter and internal bremsstrahlung," *Journal of Cosmology and Astroparticle Physics*, vol. 2014, no. 04, p. 022, 2014.

[81] Y. Bai and J. Berger, "Lepton portal dark matter," *Journal of High Energy Physics*, vol. 2014, no. 8, p. 153, 2014.

[82] Y. Farzan and J. Heeck, "Neutrinophilic nonstandard interactions," *Physical Review D*, vol. 94, no. 5, p. 053010, 2016.

[83] T. Kibble, "Kinematics of general scattering processes and the mandelstam representation," *Physical Review*, vol. 117, no. 4, p. 1159, 1960.

[84] V. Berestetskii, E. Lifshitz, and V. Pitaevskii, "Relativistic quantum theory. pt. 1," *Course of theoretical physics-Pergamon International Library of Science, Technology, Engineering & Social Studies, Oxford: Pergamon Press, 1971, edited by Landau, Lev Davidovich (series); Lifshitz, EM (series)*, pp. 218–225, 1971.

[85] F. Giacchino, L. Lopez-Honorez, and M. Tytgat, "Scalar dark matter models with significant internal bremsstrahlung j. cosmol," *Astropart. Phys*, vol. 10, no. 025, pp. 1307–6480, 2013.

[86] K. Griest and D. Seckel, "Three exceptions in the calculation of relic abundances," *Physical Review D*, vol. 43, no. 10, p. 3191, 1991.

[87] C. Boehm, P. Fayet, and R. Schaeffer, "Constraining dark matter candidates from structure formation," *Physics Letters B*, vol. 518, no. 1-2, pp. 8–14, 2001.

[88] G. Mangano, A. Melchiorri, P. Serra, A. Cooray, and M. Kamionkowski, "Cosmological bounds on dark-matter-neutrino interactions," *Physical Review D*, vol. 74, no. 4, p. 043517, 2006.

[89] C. Boehm and R. Schaeffer, "Constraints on dark matter interactions from structure formation: Damping lengths," *Astronomy & Astrophysics*, vol. 438, no. 2, pp. 419–442, 2005.

[90] C. Boehm, A. Riazuelo, S. H. Hansen, and R. Schaeffer, "Interacting dark matter disguised as warm dark matter," *Physical Review D*, vol. 66, no. 8, p. 083505, 2002.

[91] M. Escudero, O. Mena, A. C. Vincent, R. J. Wilkinson, and C. Bœhm, "Exploring dark matter microphysics with galaxy surveys," *Journal of Cosmology and Astroparticle Physics*, vol. 2015, no. 09, p. 034, 2015.

[92] M. Viel, G. D. Becker, J. S. Bolton, and M. G. Haehnelt, "Warm dark matter as a solution to the small scale crisis: New constraints from high redshift lyman-α forest data," *Physical Review D*, vol. 88, no. 4, p. 043502, 2013.

[93] R. J. Wilkinson, C. Boehm, and J. Lesgourgues, "Constraining dark matter-neutrino interactions using the cmb and large-scale structure," *Journal of Cosmology and Astroparticle Physics*, vol. 2014, no. 05, p. 011, 2014.

[94] S. Hannestad, "What is the lowest possible reheating temperature?," *Physical Review D*, vol. 70, no. 4, p. 043506, 2004.

[95] K. Enqvist, K. Kainulainen, and V. Semikoz, "Neutrino annihilation in hot plasma," *Nuclear Physics B*, vol. 374, no. 2, pp. 392–404, 1992.

[96] C. Boehm, M. J. Dolan, and C. McCabe, "A lower bound on the mass of cold thermal dark matter from planck," *Journal of Cosmology and Astroparticle Physics*, vol. 2013, no. 08, p. 041, 2013.

[97] R. J. Wilkinson, A. C. Vincent, C. Bœhm, and C. McCabe, "Ruling out the light weakly interacting massive particle explanation of the galactic 511 kev line," *Physical Review D*, vol. 94, no. 10, p. 103525, 2016.

[98] S. Chang, R. Edezhath, J. Hutchinson, and M. Luty, "Leptophilic effective wimps," *Physical Review D*, vol. 90, no. 1, p. 015011, 2014.

[99] R. Agnese, A. Anderson, M. Asai, D. Balakishiyeva, R. B. Thakur, D. Bauer, J. Billard, A. Borgland, M. Bowles, D. Brandt, *et al.*, "Search for low-mass weakly interacting massive particles using voltage-assisted calorimetric ionization detection in the supercdms experiment," *Physical review letters*, vol. 112, no. 4, p. 041302, 2014.

[100] D. S. Akerib, H. Araújo, X. Bai, A. Bailey, J. Balajthy, S. Bedikian, E. Bernard, A. Bernstein, A. Bolozdynya, A. Bradley, *et al.*, "First results from the lux dark matter experiment at the sanford underground research facility," *Physical review letters*, vol. 112, no. 9, p. 091303, 2014.

[101] J. H. Davis, "The past and future of light dark matter direct detection," *International Journal of Modern Physics A*, vol. 30, no. 15, p. 1530038, 2015.

[102] Z. Ahmed, C. collaboration, *et al.*, "Results from the final exposure of the cdms ii experiment," *arXiv preprint arXiv:0912.3592*, 2009.

[103] R. Bernabei, P. Belli, F. Cappella, V. Caracciolo, S. Castellano, R. Cerulli, C. Dai, A. d'Angelo, S. d'Angelo, A. Di Marco, *et al.*, "Final model independent result of dama/libra–phase1," *The European Physical Journal C*, vol. 73, no. 12, p. 2648, 2013.

[104] L. Baudis *et al.*, "Darwin dark matter wimp search with noble liquids," in *Journal of Physics: Conference Series*, vol. 375, p. 012028, IOP Publishing, 2012.

[105] D. Malling, D. Akerib, H. Araujo, X. Bai, S. Bedikian, E. Bernard, A. Bernstein, A. Bradley, S. Cahn, M. Carmona-Benitez, *et al.*, "After lux: the lz program," *arXiv preprint arXiv:1110.0103*, 2011.